Steady-state and time-dependent LPP modelling

J. White
University College Dublin

Outline

1. A steady state plasma (optically thin)

4d-4f + 4p-4d emission: statistical UTA (*gf*), ion distribution f_z = f(T_e)
n_e and pulse length (YAG and CO_2)

2. A time-dependent 1-D plasma (optically thick)

ion distribution, f_z = f(r,t), hydrodynamics [Medusa], some diagnostics
N_i, N_j level populations for radiation transport [UCD],
2 surveys: power density and pulse length (optimum laser conditions)

3. A 2-D plasma

time-dependent spectra [EPPRA, Z*]
spatial pulse shape (flat-top/Gaussian)
pulse length results

Conclusions

0. Introduction

- quantify 2% in-band emission (13.365-13.635 nm)
- source metric: F (steady-state), CE (time-integrated)

1) "optically thin" – doped tin (5% tin by number)

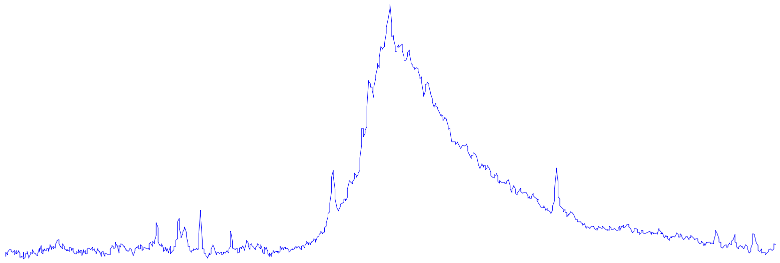

$$F = \sum_{\lambda} \sum_{z} R_{\lambda}^{n} f_z gf_{\lambda,z}$$

2) "optically thick" – pure tin

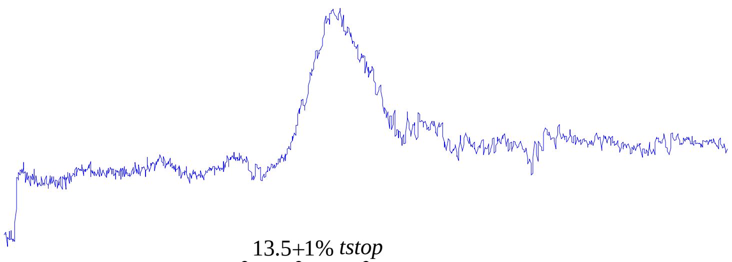

$$CE = \frac{2\pi \int \int_{13.5-1\%}^{13.5+1\%} \int_{0}^{tstop} I_{out}(\lambda,t)\,dt\,d\lambda\,dA}{E_{tot}}$$

optics
$R(\lambda)$
(2% BW)

atomic physics
UTA
gf versus λ

plasma physics
f_z versus T_e
I versus r,t

theoretical
spectra
F, CE

experimental comparisons (UCD):
Jenoptik 0.25-m grazing incidence,
1064-nm, 15-ns FWHM Nd:YAG

Outline

1. A steady state plasma (optically thin)

4d-4f + 4p-4d emission: statistical UTA (*gf*), ion distribution $f_z = \mathrm{f}(T_e)$

n_e and pulse length (YAG and CO_2)

2. A time-dependent 1-D plasma (optically thick)

ion distribution, $f_z = \mathrm{f}(r,t)$, hydrodynamics [Medusa], some diagnostics

N_i, N_j level populations for radiation transport [UCD],

2 surveys: power density and pulse length (optimum laser conditions)

3. A 2-D plasma

time-dependent spectra [EPPRA, Z*]

spatial pulse shape (flat-top/Gaussian)

pulse length results

Conclusions

1. ‘Steady-state’ (oscillators weighted by ion distribution) $gf \bullet f_z$

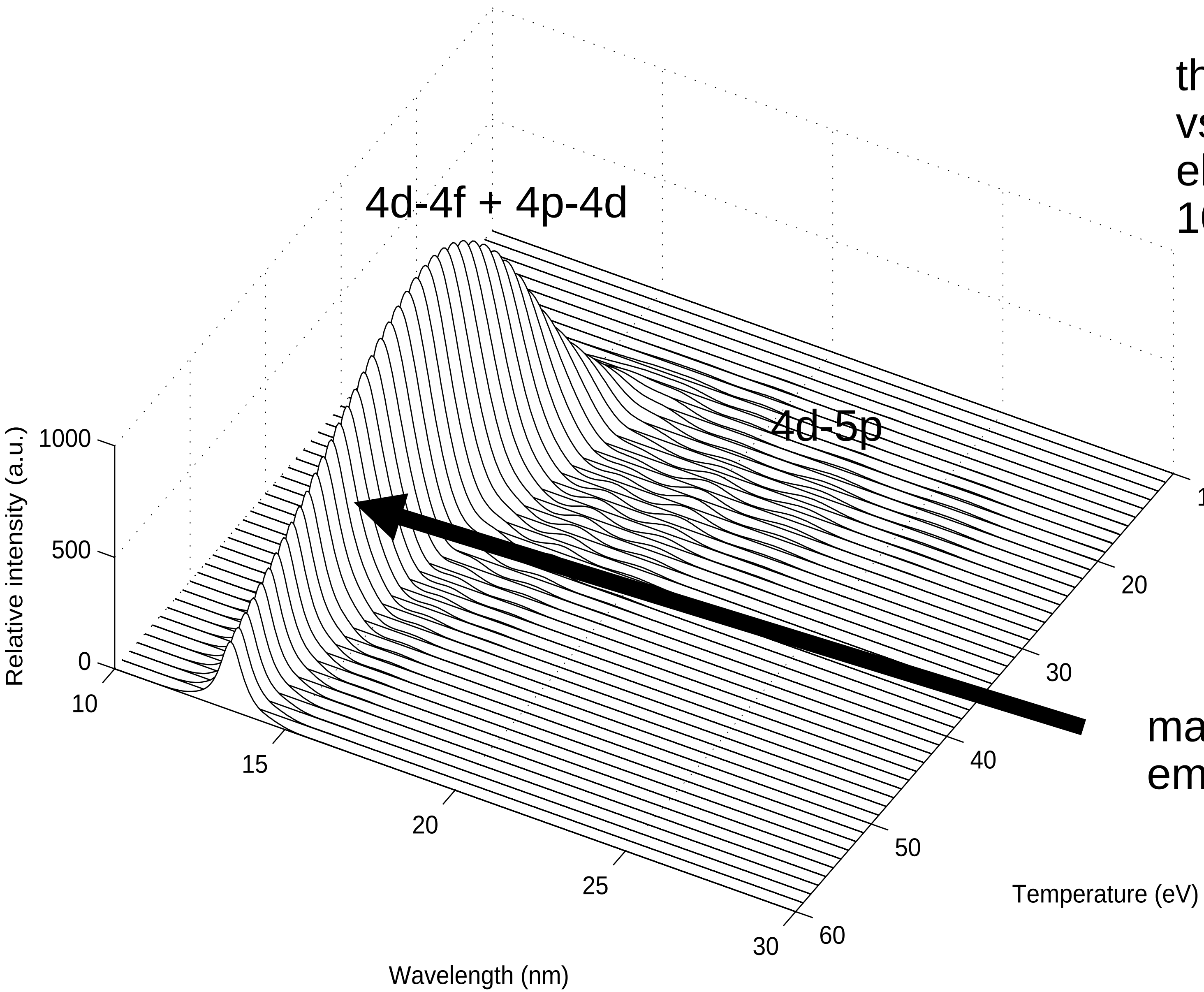

theoretical spectra vs wavelength and electron temperature 10–60 eV

maximum 13.5-nm emission at 40 eV

1. Steady-state plasma in-band contribution

- 20 eV

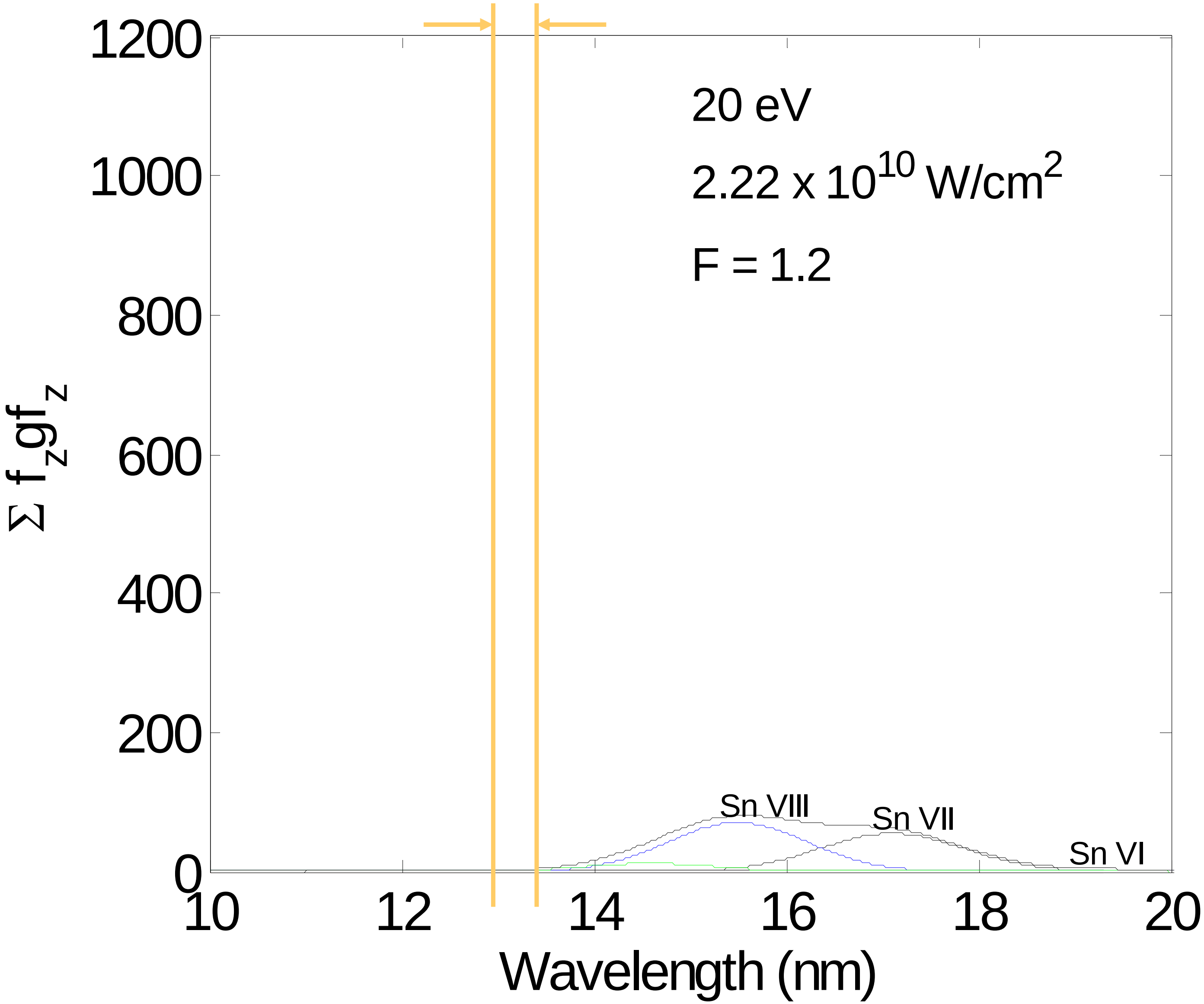

1. Steady-state plasma in-band contribution

- 30 eV

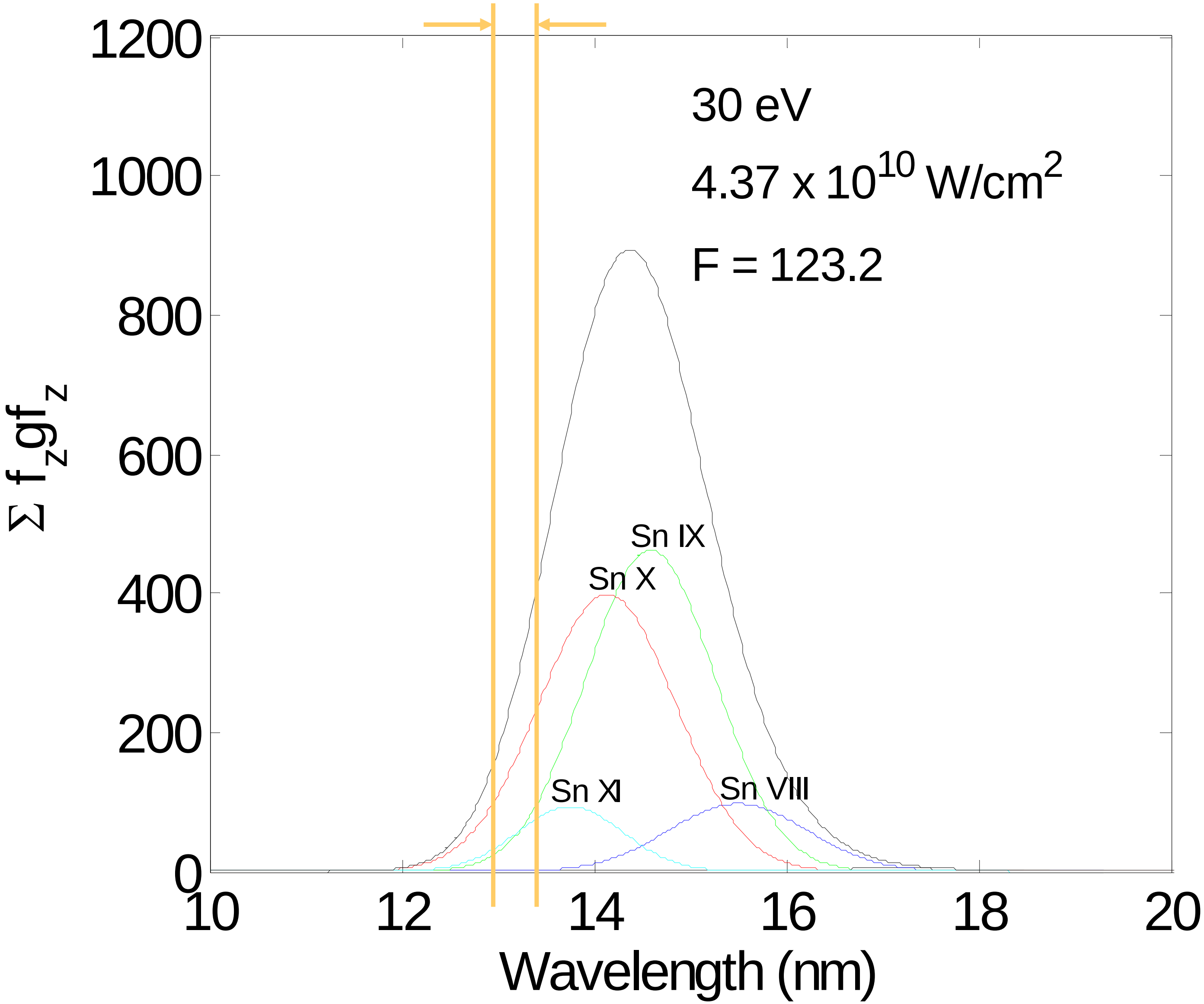

1. Steady-state plasma in-band contribution

- 40 eV

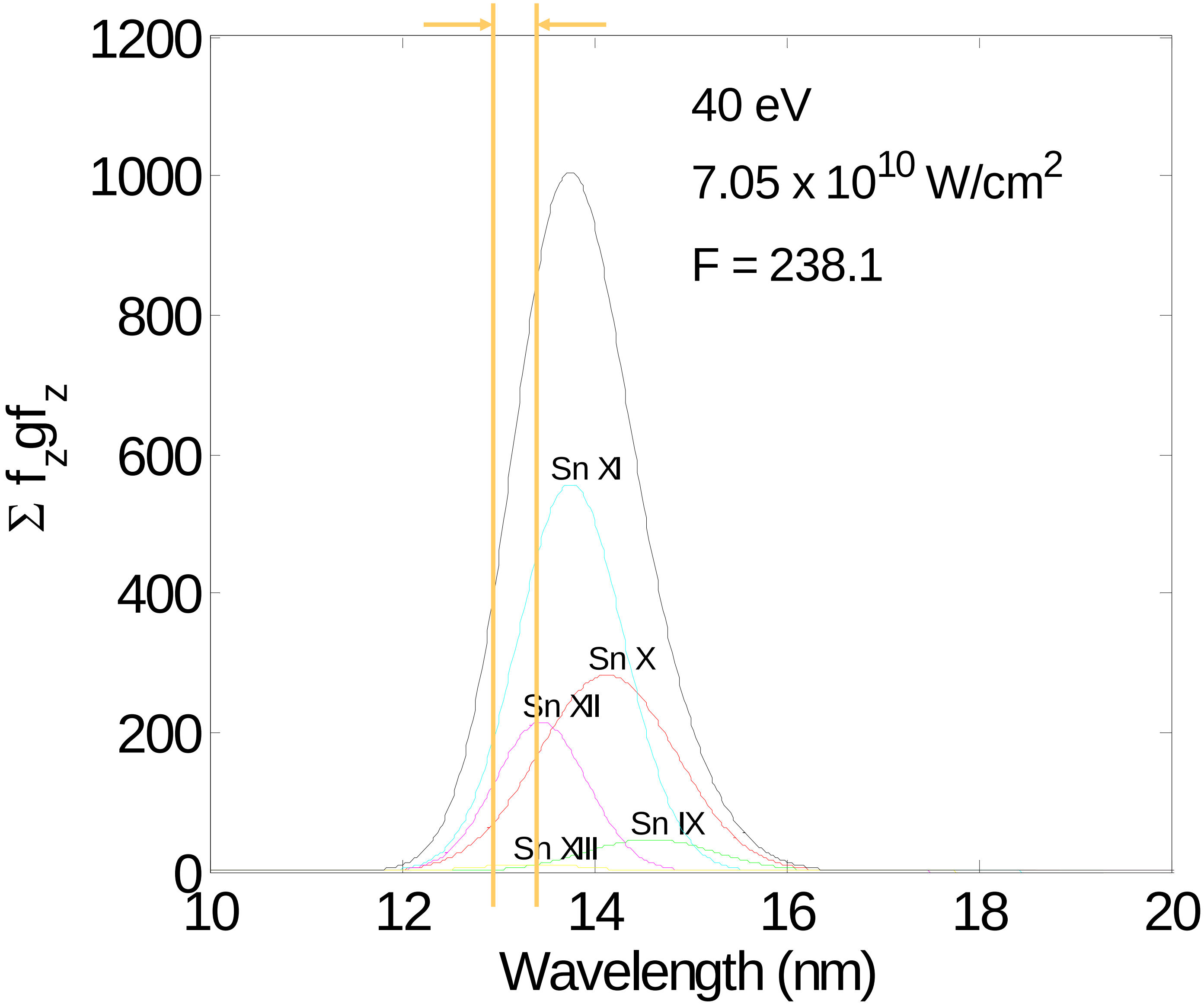

1. Steady-state plasma in-band contribution

- 50 eV

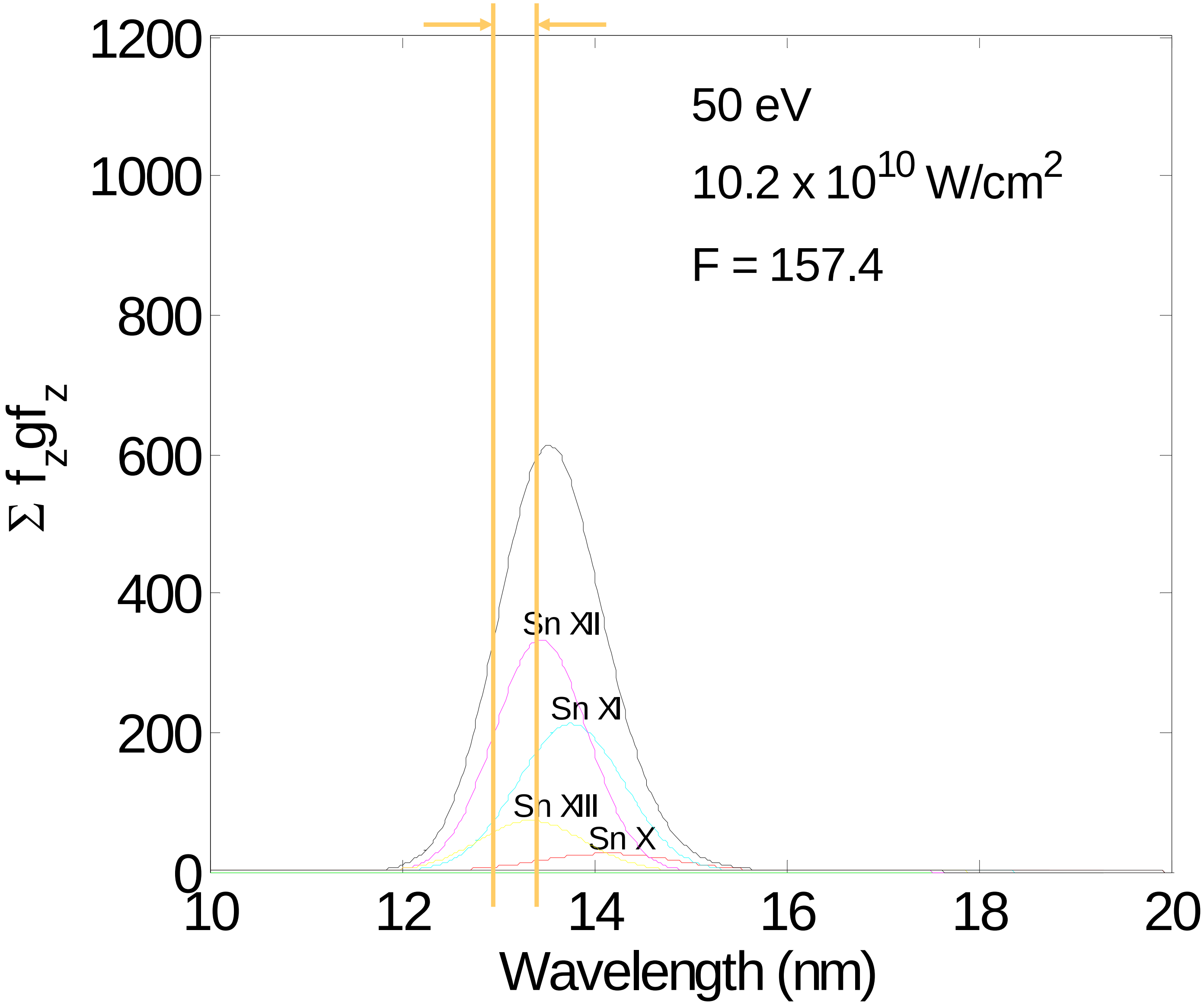

1. Steady-state plasma in-band contribution

- 60 eV

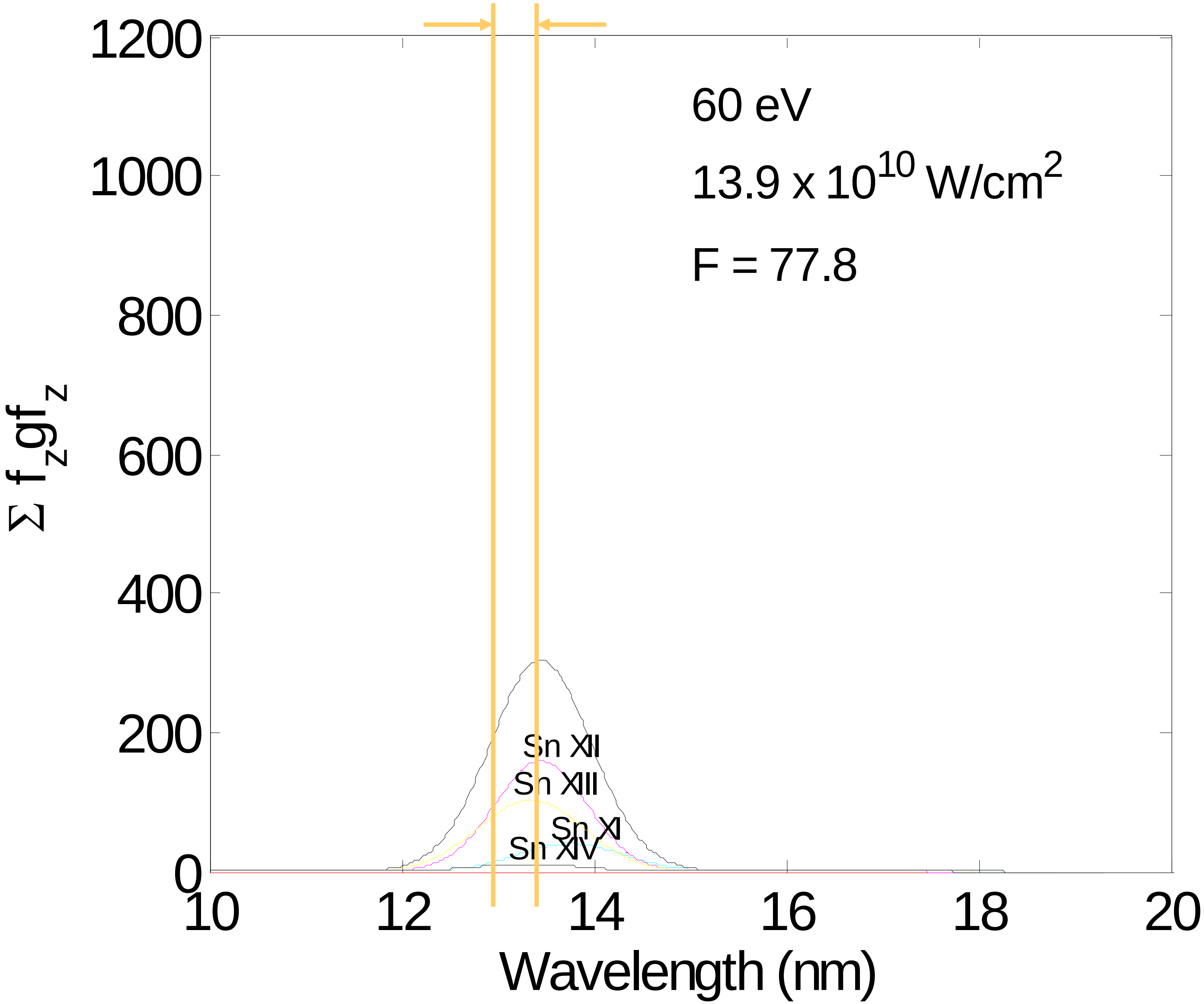

1. Steady-state plasma in-band contribution

- 70 eV

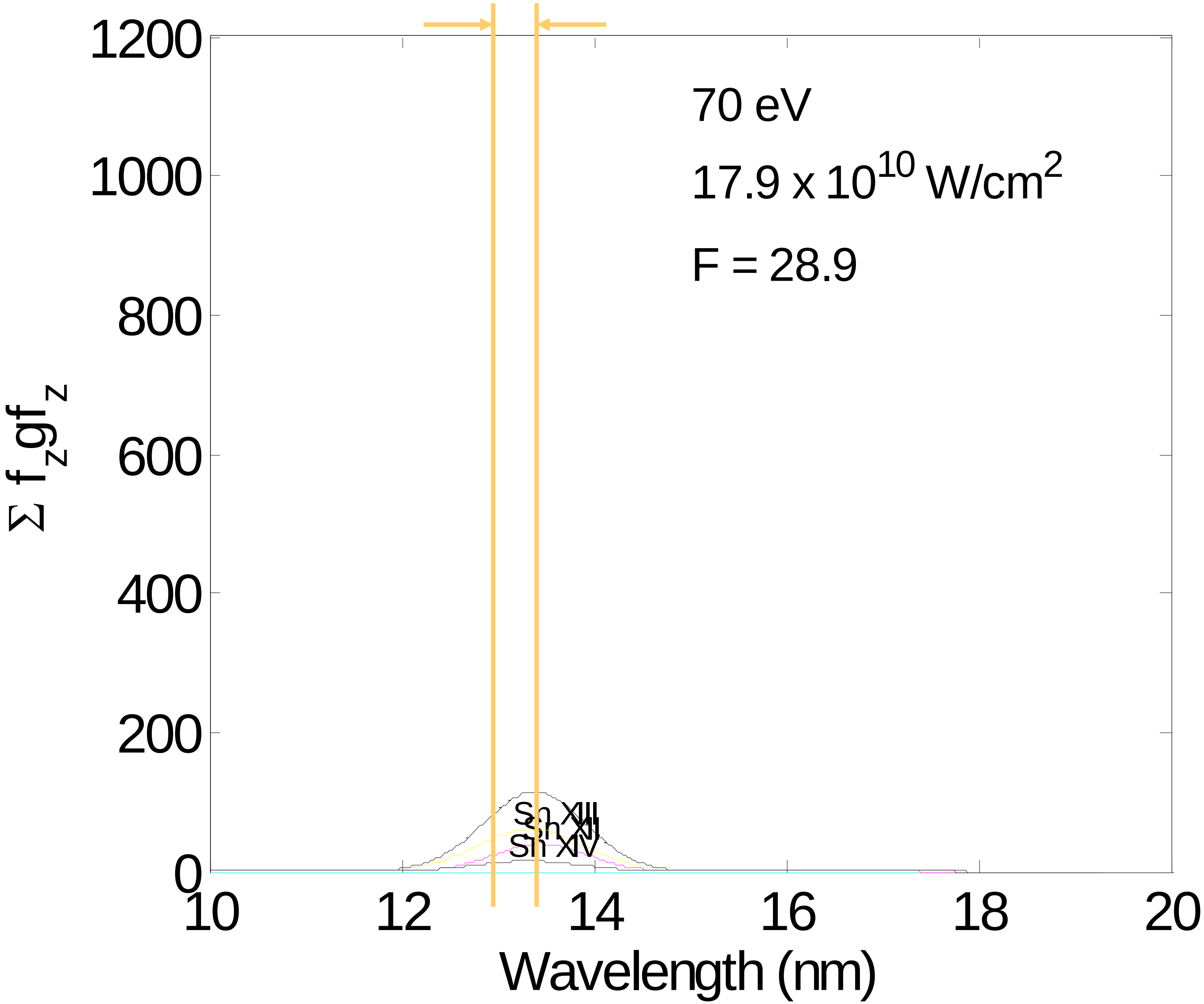

1. Experimental comparison

- long wavelength match at lower temperatures 30-35 eV

5% tin by number (optically thin)

Jenoptik 0.25-m grazing incidence flat field spectograph (UCD)

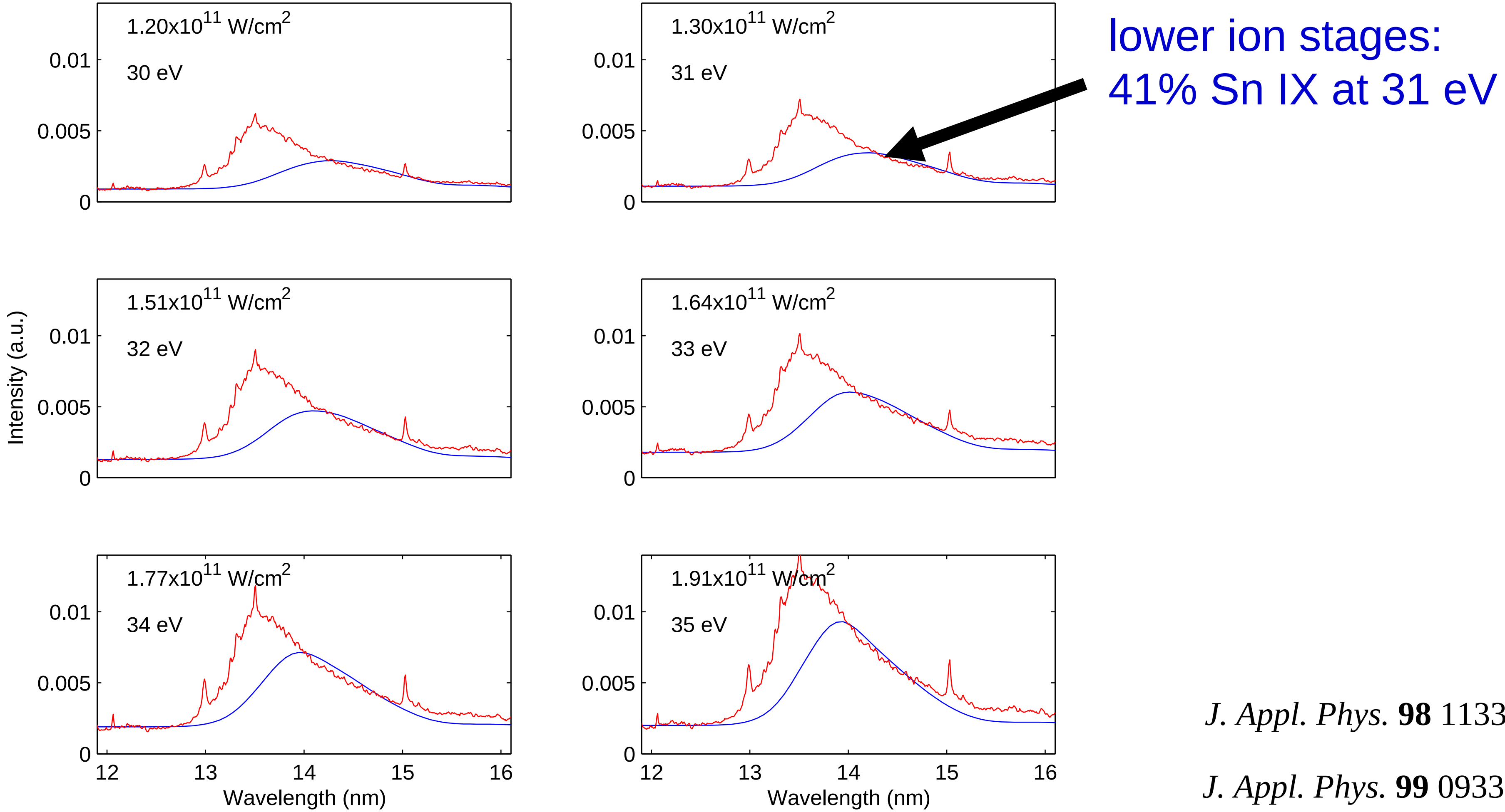

J. Appl. Phys. **98** 113301, 2005

J. Appl. Phys. **99** 093302, 2006

1. Experimental comparison

- short wavelength match at higher temperatures 43-50 eV

5% tin by number (optically thin)

Jenoptik 0.25-m grazing incidence flat field spectograph (UCD)

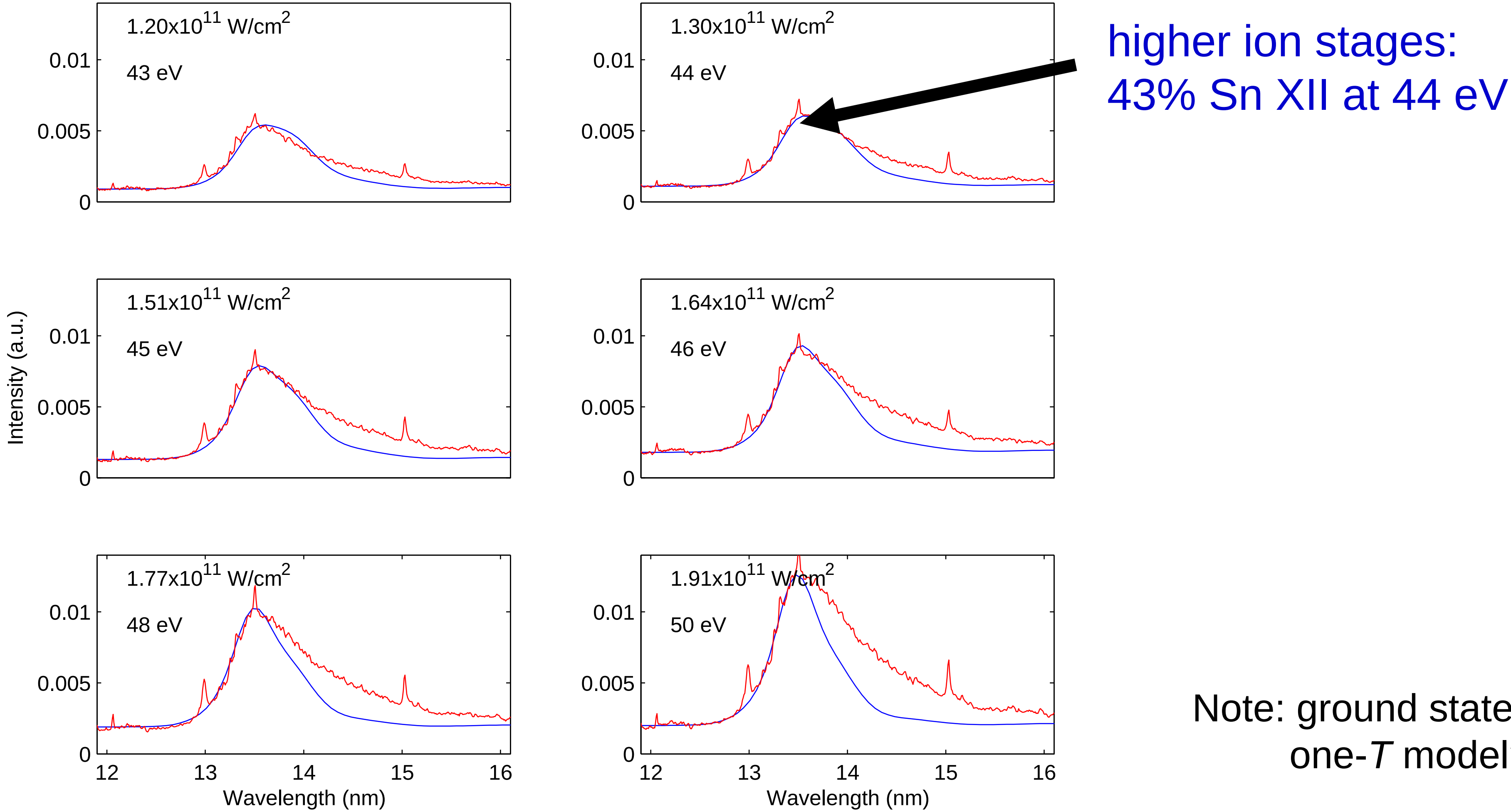

Note: ground state only one-*T* model?

1. Statistical representation '4d' subshell ions: Sn VII–Sn XIV

- **H ψ = E ψ**
  - statistical "three-parameter" Gaussian (mean, standard deviation, Σgf) versus λ

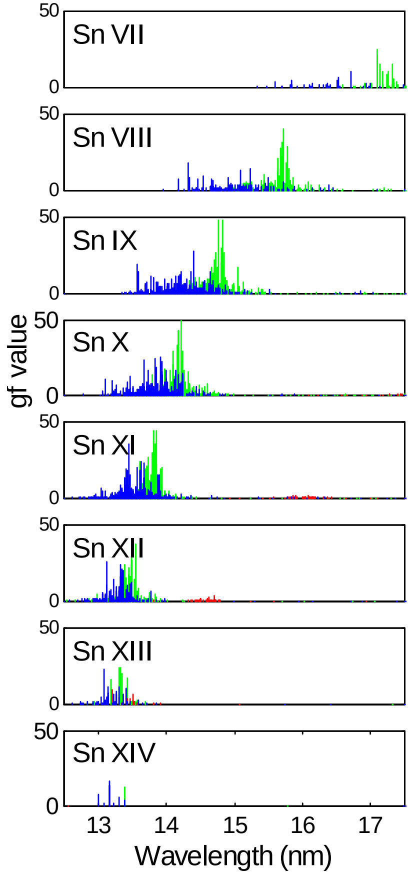

$$\mu_n = \frac{\sum_{i=1}^{N} (\lambda_i)^n gf_i}{\sum_{i=1}^{N} gf_i}$$

$$f(x) = \frac{1}{\sigma\sqrt{2\pi}} e^{-\frac{(x-\mu_1)^2}{2\sigma^2}}$$

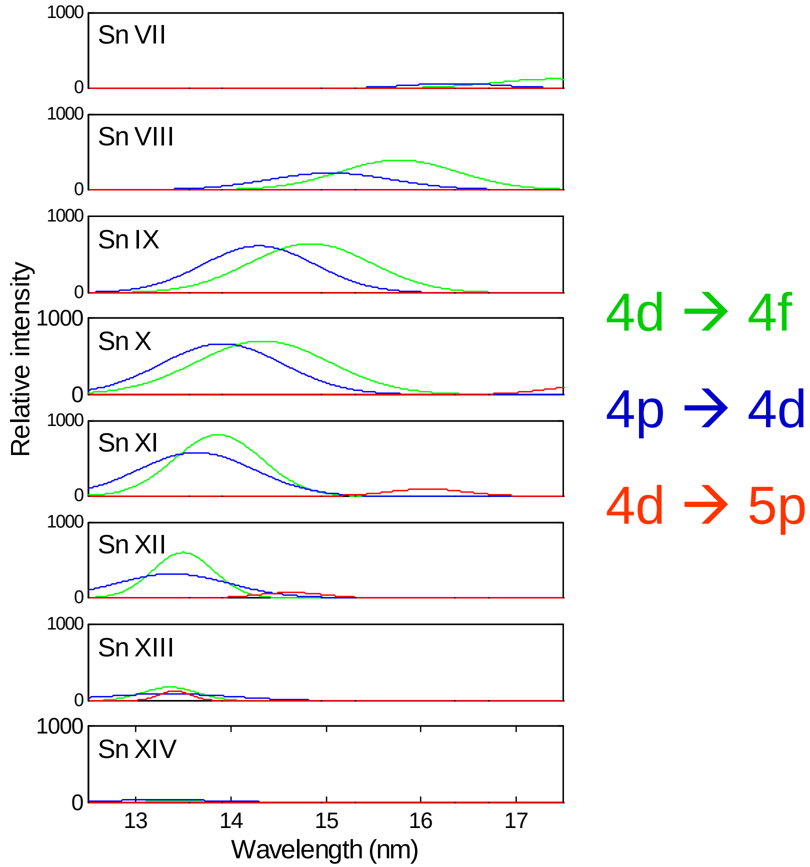

1. Rate equations: ionisation vs recombination

- ion distribution f_z from rate equations (from atomic processes)
  - collisional ionisation, S(z-1)
  - radiative recombination, α_r (z)
  - three-body recombination, α_{3b}(z)
  - semi-empirical
- a balance of ionisation and recombination

ionisation

$$f_z = \frac{S}{\alpha_r + n_e \times \alpha_{3b}}$$

recombination

$$\mathbf{S = 9 \times 10^{-6}\, \xi_z\, (T_e / \chi_z)^{1/2}\, e^{(-\chi_z / T_e)}}$$
$$\mathbf{\chi_z^{3/2}\, (4.88 + T_e / \chi_z)}$$

$$\mathbf{\alpha_r = 5.2 \times 10^{-14}\, (\chi_z / T_e)^{1/2}\, Z}$$
$$\mathbf{[0.429 + .5 \log(\chi_z / T_e) + 0.469\, (T_e / \chi_z)^{1/2}]}$$

$$\mathbf{\alpha_{3b} = 2.97 \times 10^{-27}\, \xi_z}$$
$$\mathbf{T_e\, \chi_z^2\, (4.88 + T_e / \chi_z)}$$

S = collisional ionisation,
α_r = radiative recombination,
D_j = dielectronic recombination,
α_{3b} = three-body recombination,
T_e = electron temperature,
n_e = electron density,
Z = atomic number,
χ_z = ionisation potential,
ξ_z = number of open shell electrons,
z = ion stage.

1. Nd:YAG and CO2

Appl. Phys. Lett., 90, 181502, 2007

Optimising 13.5-nm emission as a function of laser wavelength

- n_e (CO_2) = 1/100 n_e (YAG)
- lower power density to achieve 40 eV ($\lambda^2\phi$ = constant)

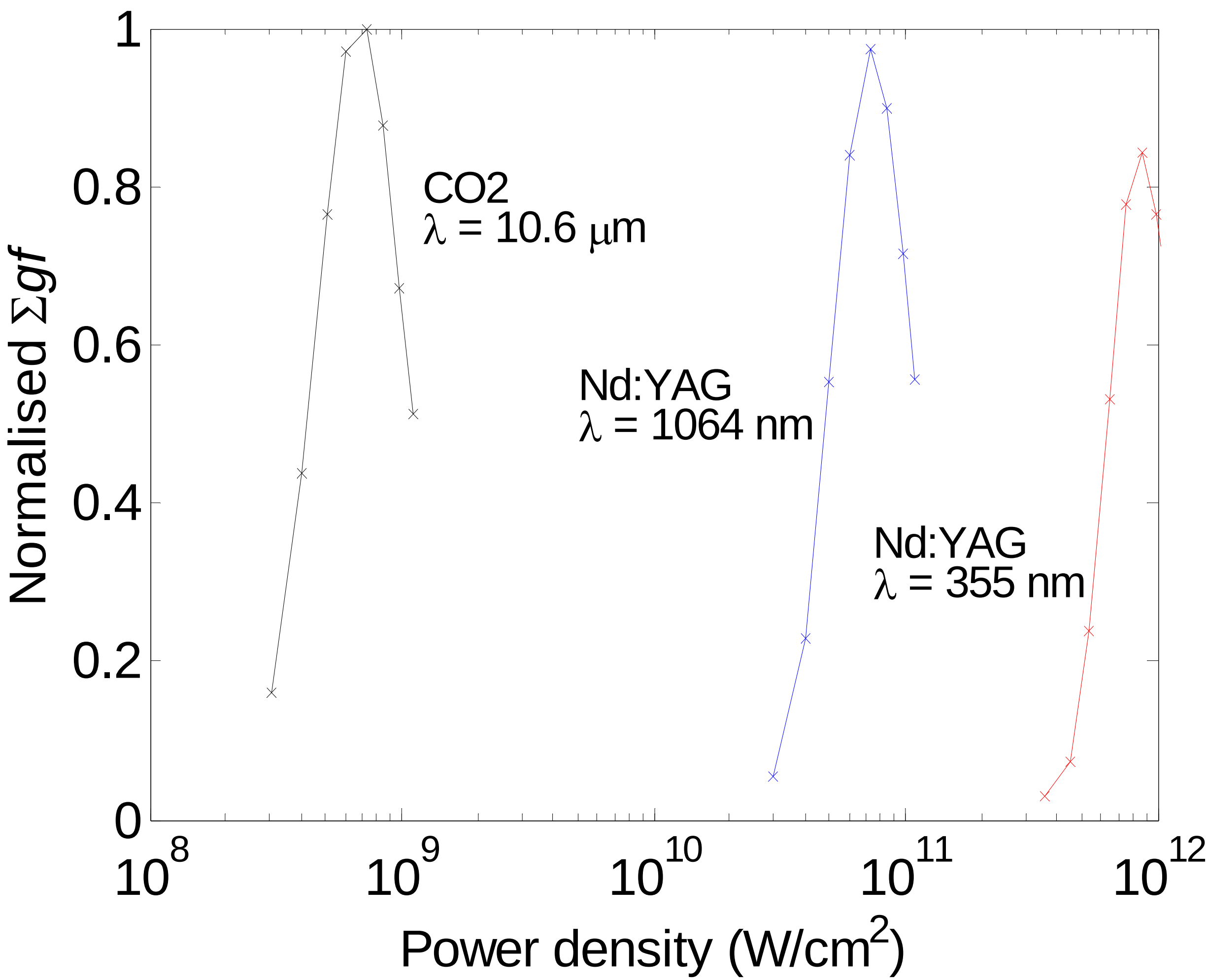

Outline

1. A steady state plasma (optically thin)

4d-4f + 4p-4d emission: statistical UTA (*gf*), ion distribution f_z = f(T_e)
n_e and pulse length (YAG and CO_2)

2. A time-dependent 1-D plasma (optically thick)

ion distribution, f_z = f(r,t), hydrodynamics [Medusa], some diagnostics
N_i, N_j level populations for radiation transport [UCD],
2 surveys: power density and pulse length (optimum laser conditions)

3. A 2-D plasma

time-dependent spectra [EPPRA, Z*]
spatial pulse shape (flat-top/Gaussian)
pulse length results

Conclusions

2. What is the emission as a function of time/space?

time-dependent plasma

dn/dt $\neq$ 0

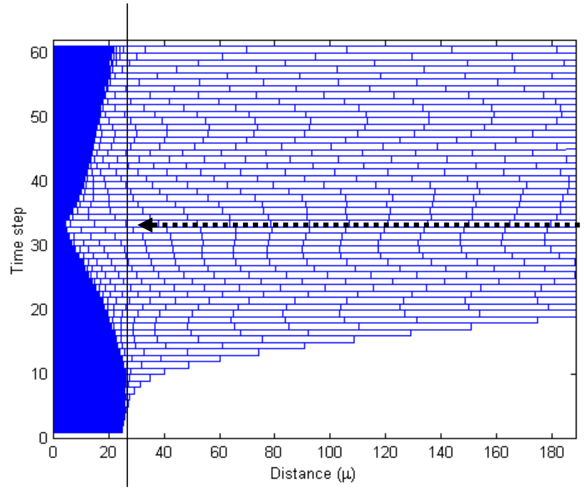

λ = 1064 nm

(Nd:YAG)

time-dependent: sharp temperature gradients

t(atomic processes) ~ t(laser)

n_e and T_e = f (r,t)

c.f. **steady-state**: one temperature

t(atomic processes) < t(laser)

$n_e = n_{ec} \approx 10^{21}\lambda^{-2}$ and $T_e \propto Z^{1/5}(\lambda^2\phi)^{3/5}$

- FORTRAN laser-plasma interaction code Medusa
- one-dimensional **Lagrangian** difference mesh
- hydrodynamics variables: **density** (ρ), **velocity** (v), **ion temperature** (T_i), **electron temperature** (T_e) as functions of **space** (r) and **time** (t) from Navier-Stokes equations
- **average atom model** (to simpify rate equations especially for high Z). P_n = n shell occupation number.
- excitation/de-excitation included (l-degenerate level populations calculated from average atom model)

2. Sn hydrodynamics: vs (*r*,*t*)

laser: $\mathbf{P_{equiv} = 1.3 \times 10^{11}\ W/cm^2}$
target: solid tin, 50 μm-diameter wire
simulation: 400 cells, 100 ns, cylindrical geometry

versus cell at: 18, 23, 28 ns (POP: 23 ns) 15-ns FWHM

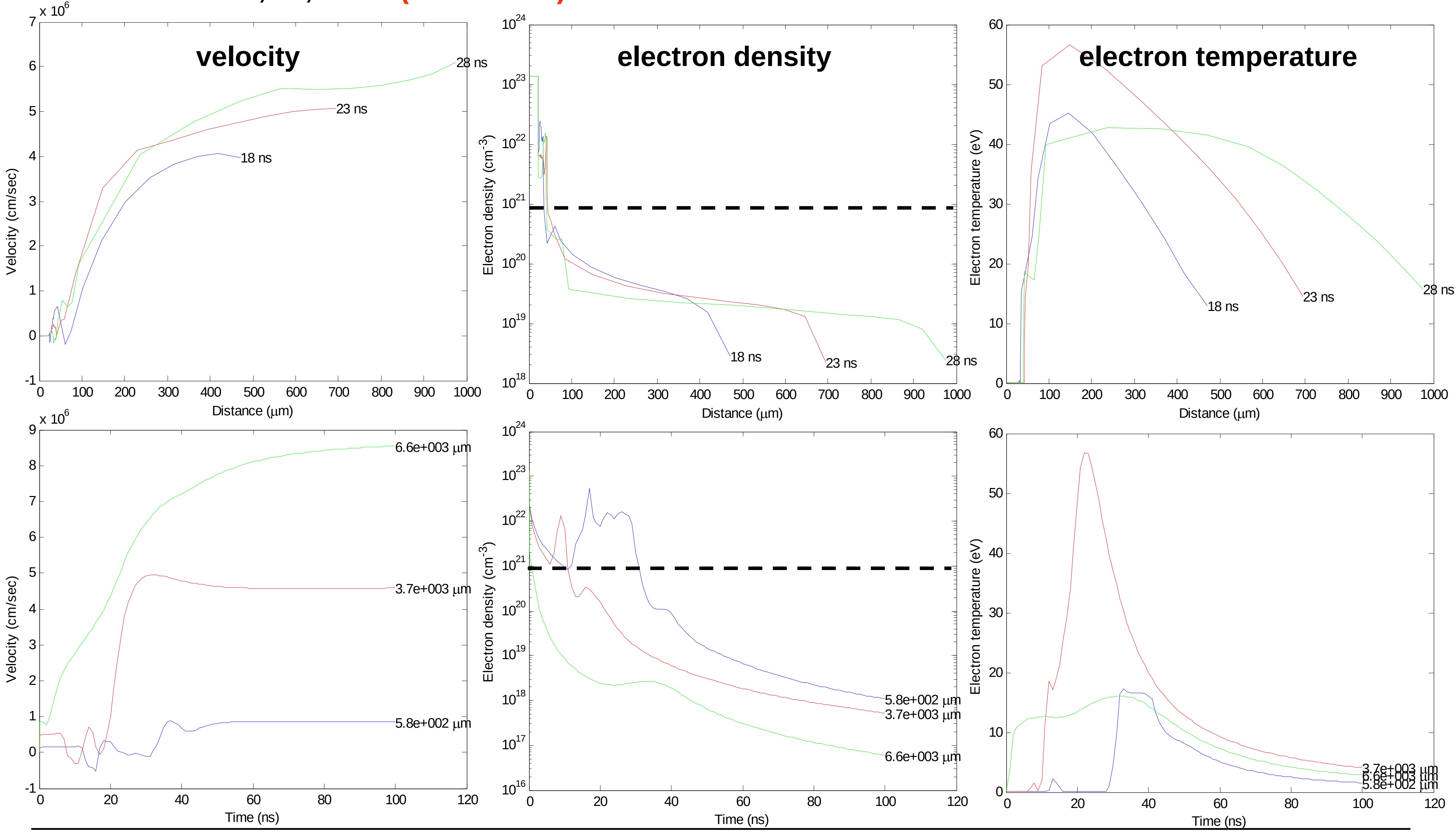

versus time at: 400, 392, 384

2. Ion distribution = f(*r*,*t*) 1-D x time Peak of the pulse

- Sn^{4+} -- Sn^{13+} ion fraction and ion density (cm^{-3})

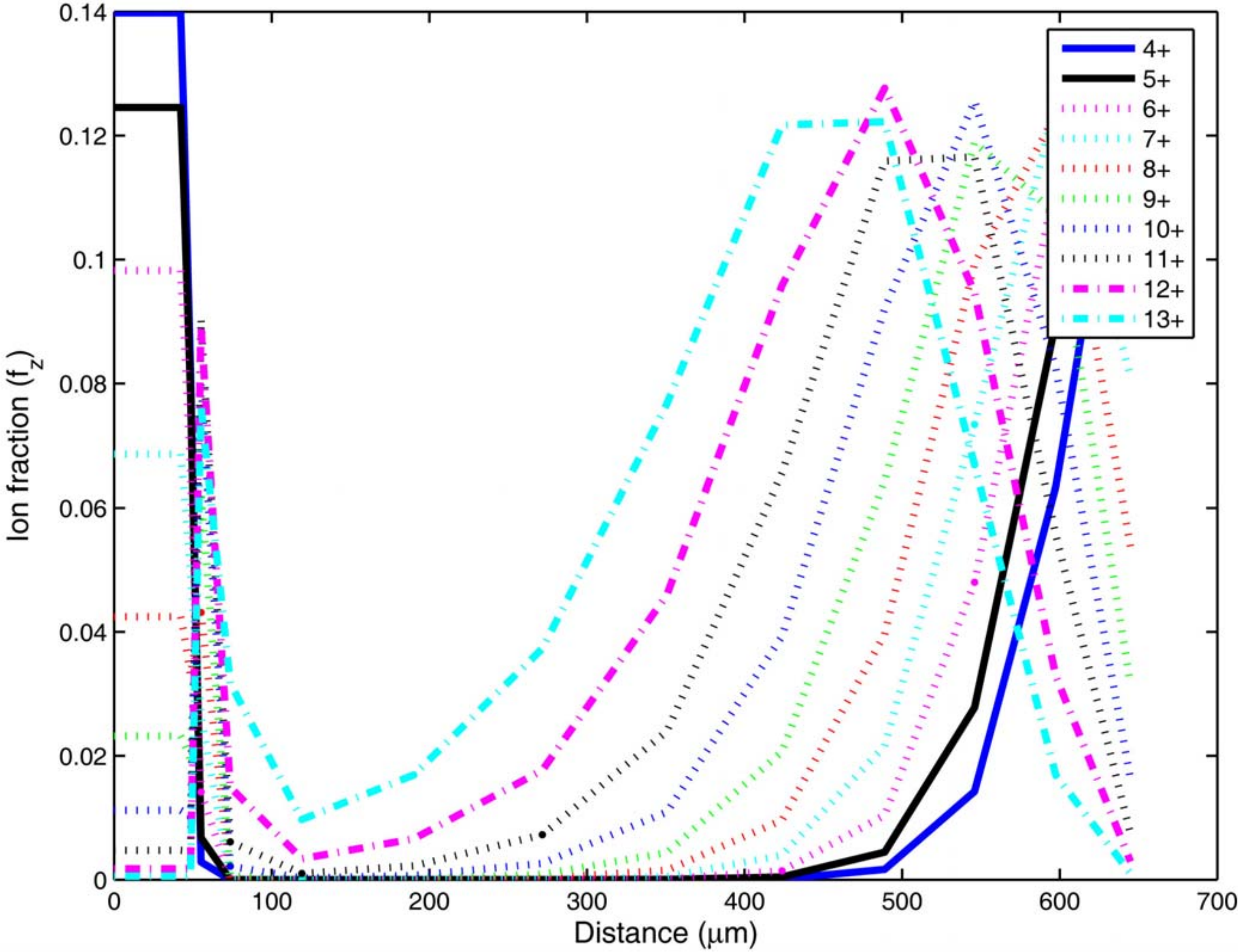

target

2. Time-dependent plasma: Sn level populations (for Δn = 0)

- Sn V – Sn XIV UTA (*l* degeneracy removed with energy functional)

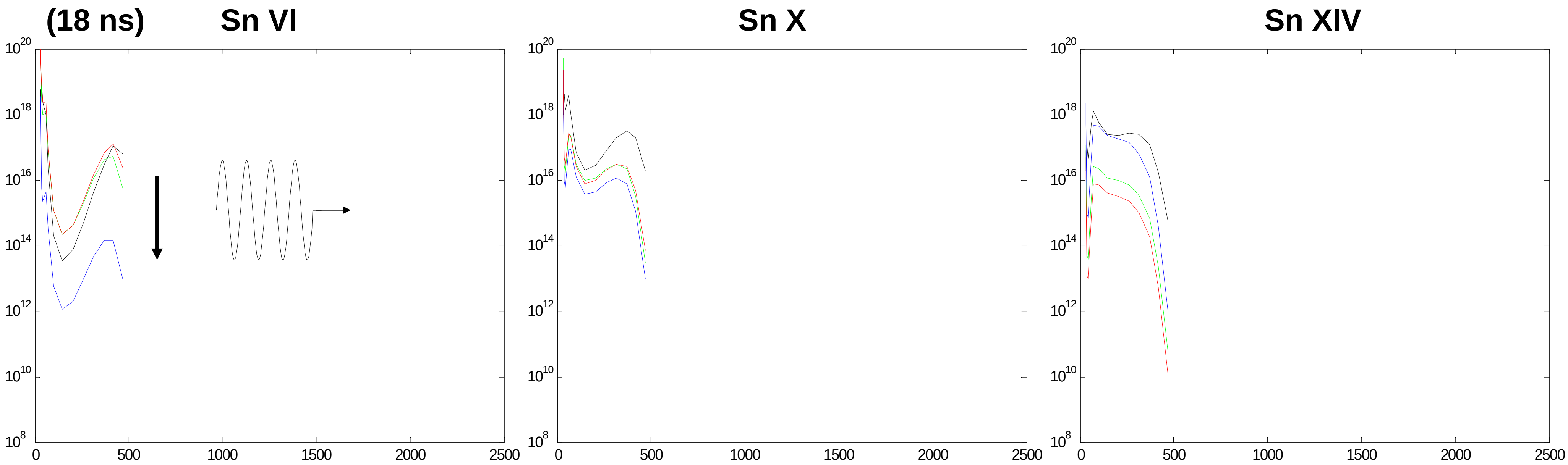

Population number densities (N_i, N_j) cm^3 versus distance (μm)

***E_0*:** black: $4p^6 4d^N$
green: $4p^6 4d^{N-1} 4f^1$
blue: $4p^5 4d^{N+1}$
red: $4p^6 4d^{N-1} 5p^1$

J. Appl. Phys. **101** 043301, 2007

2. Time-dependent plasma: Sn level populations (for $\Delta n = 0$)

- Sn V – Sn XIV UTA (*l* degeneracy removed with energy functional)

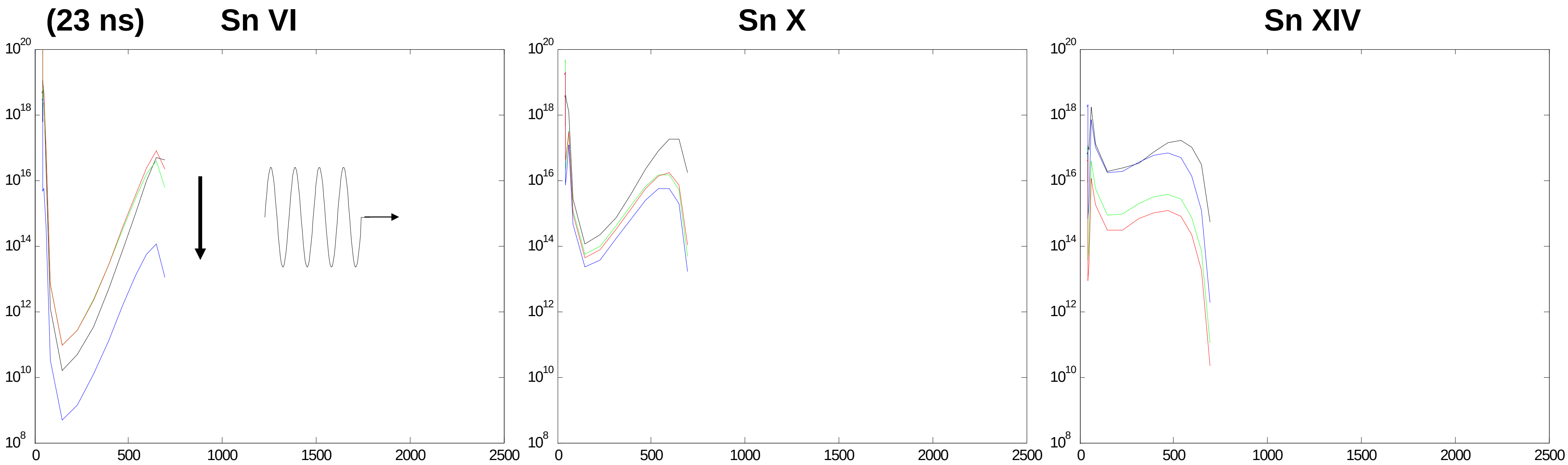

Population number densities (N_i, N_j) cm^3 versus distance (μm)

***E₀*:** black: $4p^6 4d^N$
green: $4p^6 4d^{N-1} 4f^1$
blue: $4p^5 4d^{N+1}$
red: $4p^6 4d^{N-1} 5p^1$

J. Appl. Phys. **101** 043301, 2007

2. Time-dependent plasma: Sn level populations (for $\Delta n = 0$)

- Sn V – Sn XIV UTA (*l* degeneracy removed with energy functional)

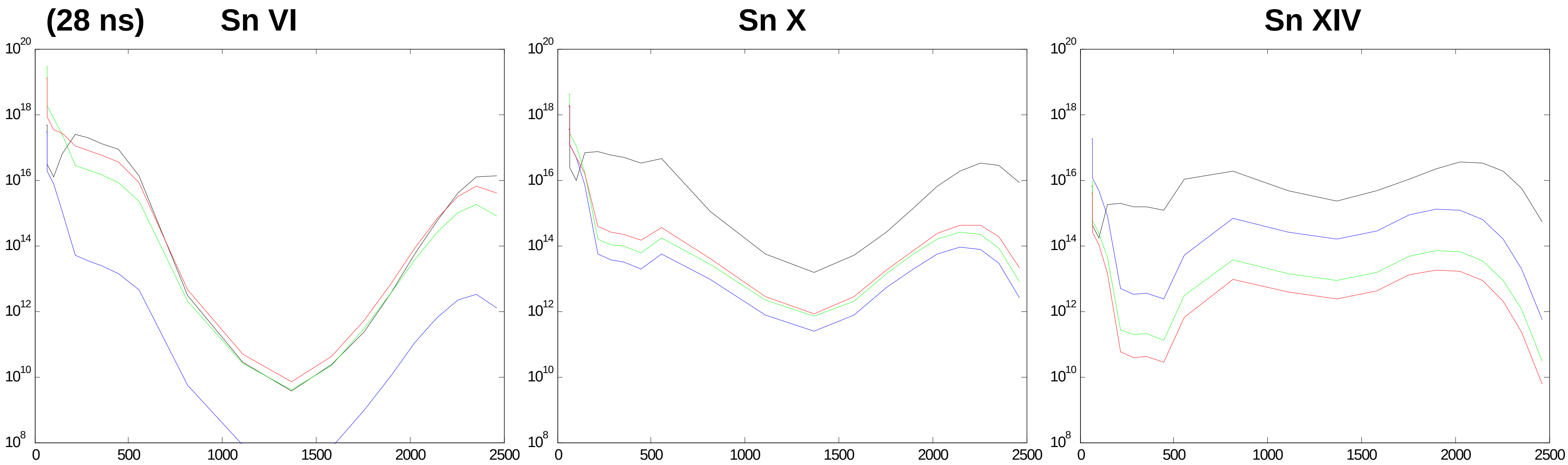

Population number densities (N_i, N_j) cm^3 versus distance (μm)

***E_0*:** black: $4p^6 4d^N$
green: $4p^6 4d^{N-1} 4f^1$
blue: $4p^5 4d^{N+1}$
red: $4p^6 4d^{N-1} 5p^1$

J. Appl. Phys. **101** 043301, 2007

2. All together: sum up intensity with absorption

- $I_m = f(r,t) \rightarrow I = f(\lambda,t)$
- absorption strength, f_{ij} (Cowan, stat UTA) $f_{ij} = \dfrac{gf}{D_i}$
- level populations, N_{ij} (Medusa, E. F.) $N_{ij} = W_a \dfrac{\rho}{Am_p}$
- degeneracy, g or D
- cell width, Δz (Medusa)
- absorption cross section, χ

$$I_m^{obs}(\nu) = I_m(\nu)\exp\left(\sum -\chi_n(\nu)\Delta z_n\right)$$

$$\chi_m^l(\nu) = \frac{\pi e^2}{4\pi\varepsilon_0 m_e c} f_{ij} N_i \left[1 - \frac{N_j g_i}{N_i g_j}\right]\phi_m^l(\nu)$$

$$I_m(\nu) = \sum_l S_m^l(\nu)[1 - \exp(\chi_m^l(\nu)\Delta z_m)]$$

$$S_m^l(\nu) = \frac{2h\nu^3}{c^2}\frac{1}{\left[\frac{N_i g_j}{N_j g_i} - 1\right]}$$

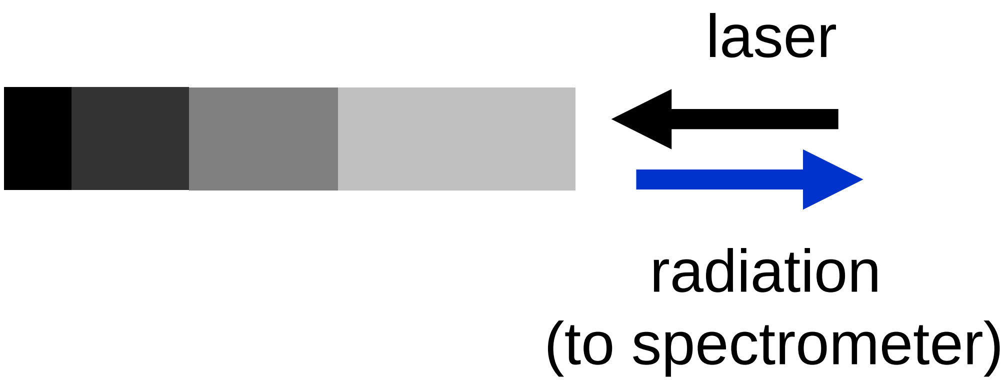

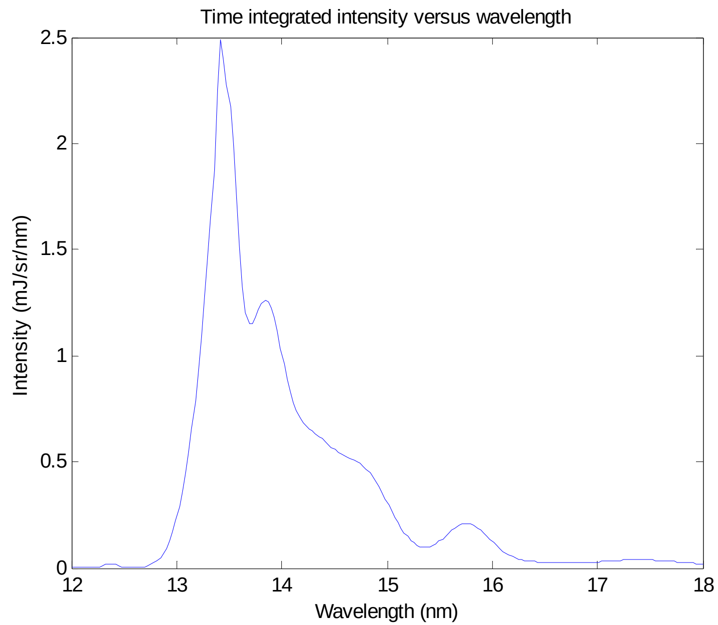

The emission as a function of time, I_{out}, is calculated by summing up attenuated cell emission over all m cells

nl level populations as a function of *r,t*

for $4p^6\,4d^N$, $4p^6 4d^{N-1} 4f^1$, $4p^5 4d^N$, and $4p^6 4d^{N-1} 5p^1$ configurations

The rest is atomic accounting (*a.k.a.* computational physics)

10 ions
3 transitions
6 shells (SHM)
400 x 400 cells (summed attenuated absorption)
or 200 x 401 = 80200 cells
100 timesteps
200 frequency points in 2% bandwidth
--
~ 3×10^{11} (300 billion) calculations/spectrum

But the good news: only 3 UTA transitions instead of 100,000 in the line-by-line analysis

So 300 billion calculations/spectrum instead of 10 thousand trillion!

2. Sn time-integrated UTA spectra

laser: 1.064 μm, 15.0 ns (FWHM), Gaussian
target: solid tin, 90 μm-diameter wire
simulation: 400 cells, 100 ns, cylindrical geometry

- power density from 0.5 to 3.0 x 10^{11} W/cm^2

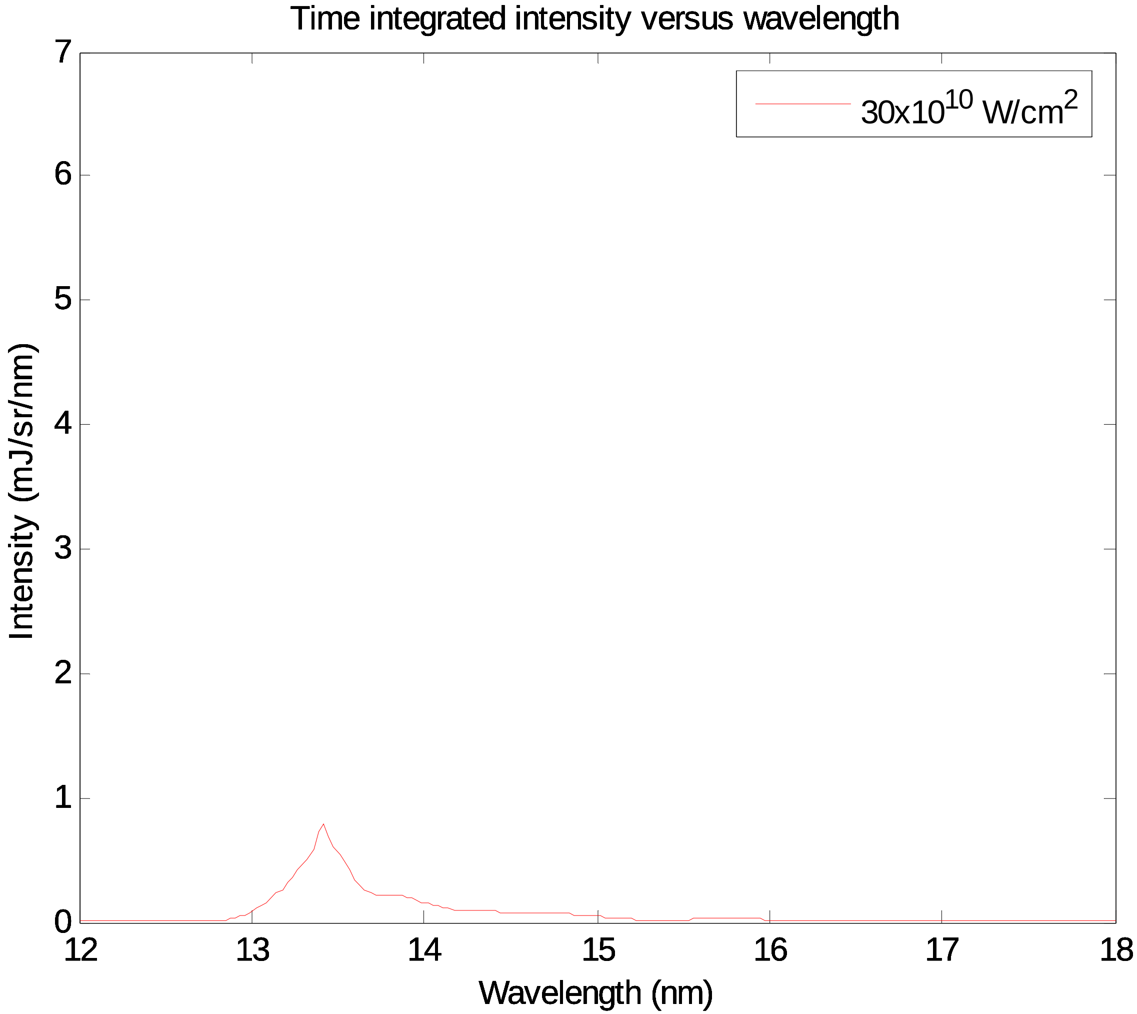

Calculated spectra: intensity versus wavelength

2. Sn UTA spectra versus time

laser: 1.064 μm, 15.0 ns (FWHM), Gaussian
target: solid tin, 90 μm-diameter wire
simulation: 400 cells, 100 ns, cylindrical geometry

- power density from 0.5 to 3.0 x 10^{11} W/cm^2

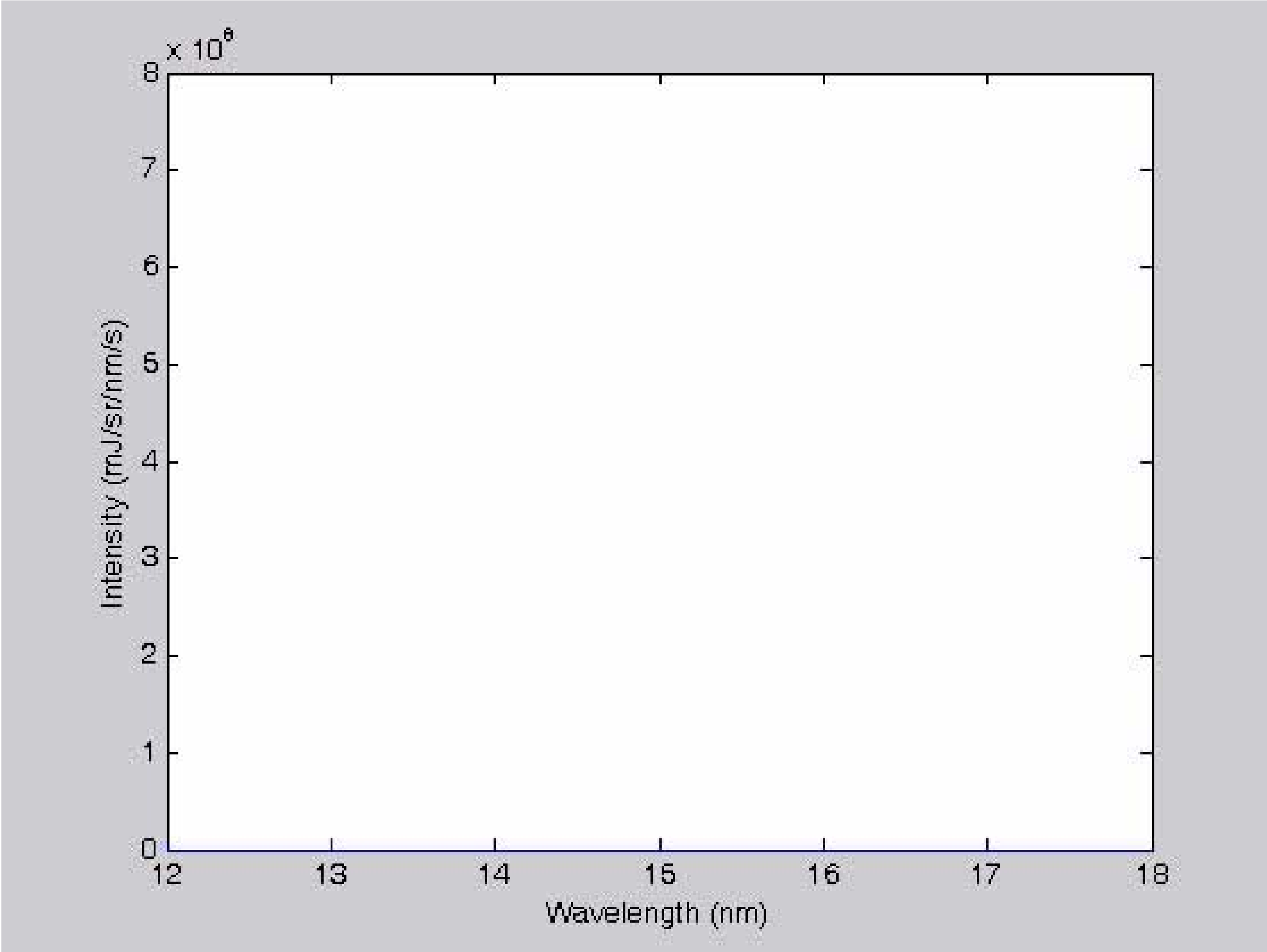

2. Sn time-integrated UTA spectra

laser: 1.064 μm, 15.0 ns (FWHM), Gaussian
target: solid tin, 90 μm-diameter wire
simulation: 400 cells, 100 ns, cylindrical geometry

- power density from 0.5 to 3.0 x 10^{11} W/cm^2: max CE at 0.8 x 10^{11} W/cm^2
- pulse width from 7 to 23 ns: max CE for 10-ns FWHM (4% > than at 15-ns)

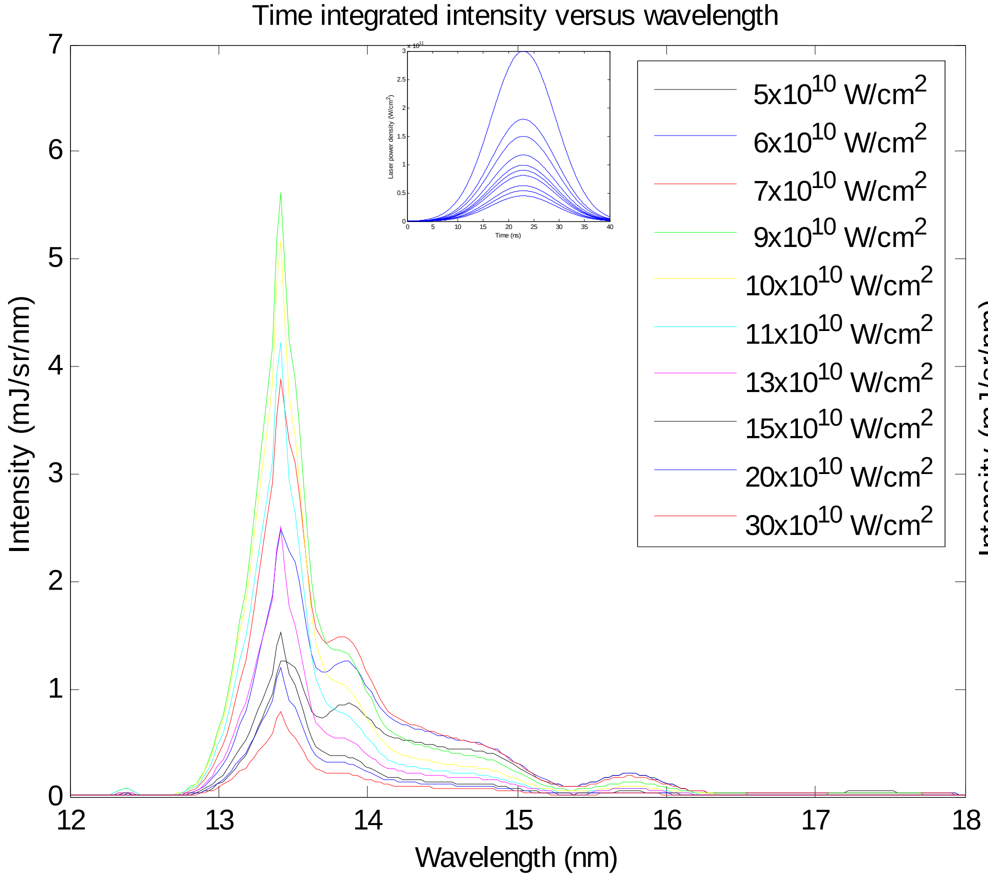

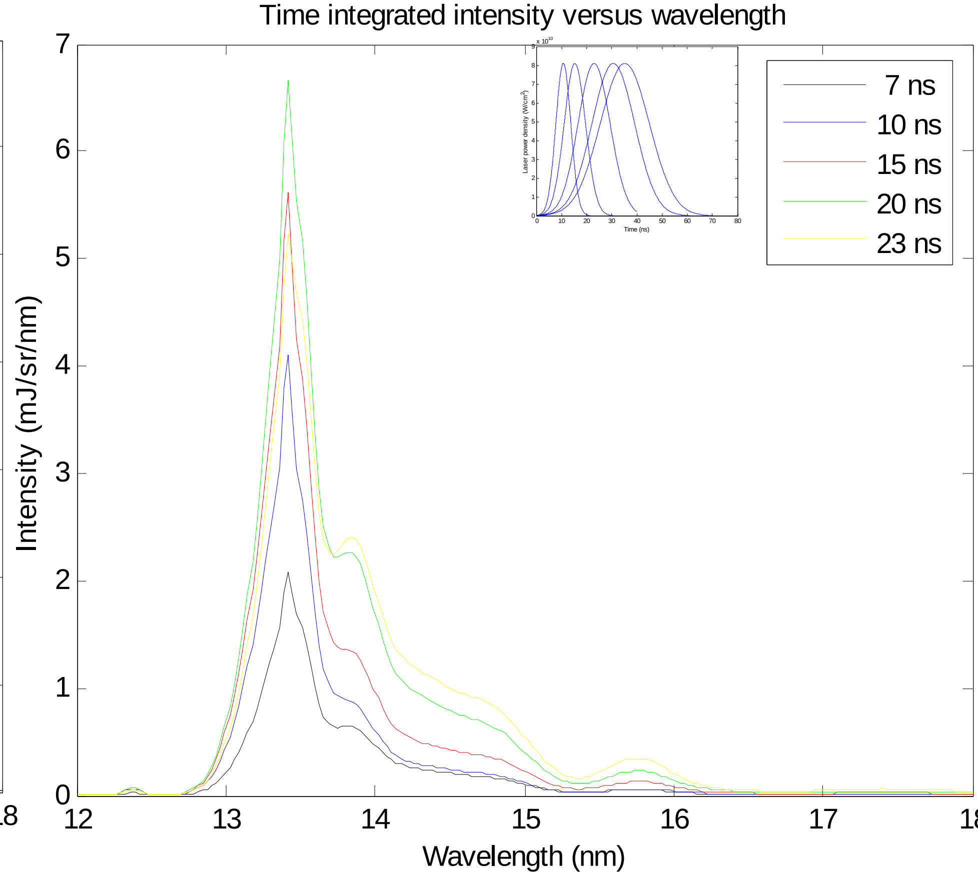

Calculated spectra: intensity versus wavelength

2. Experimental comparison

- Calculated: 0.8 x 10^{11} W/cm^2
- Experimental: 0.9 x 10^{11} W/cm^2

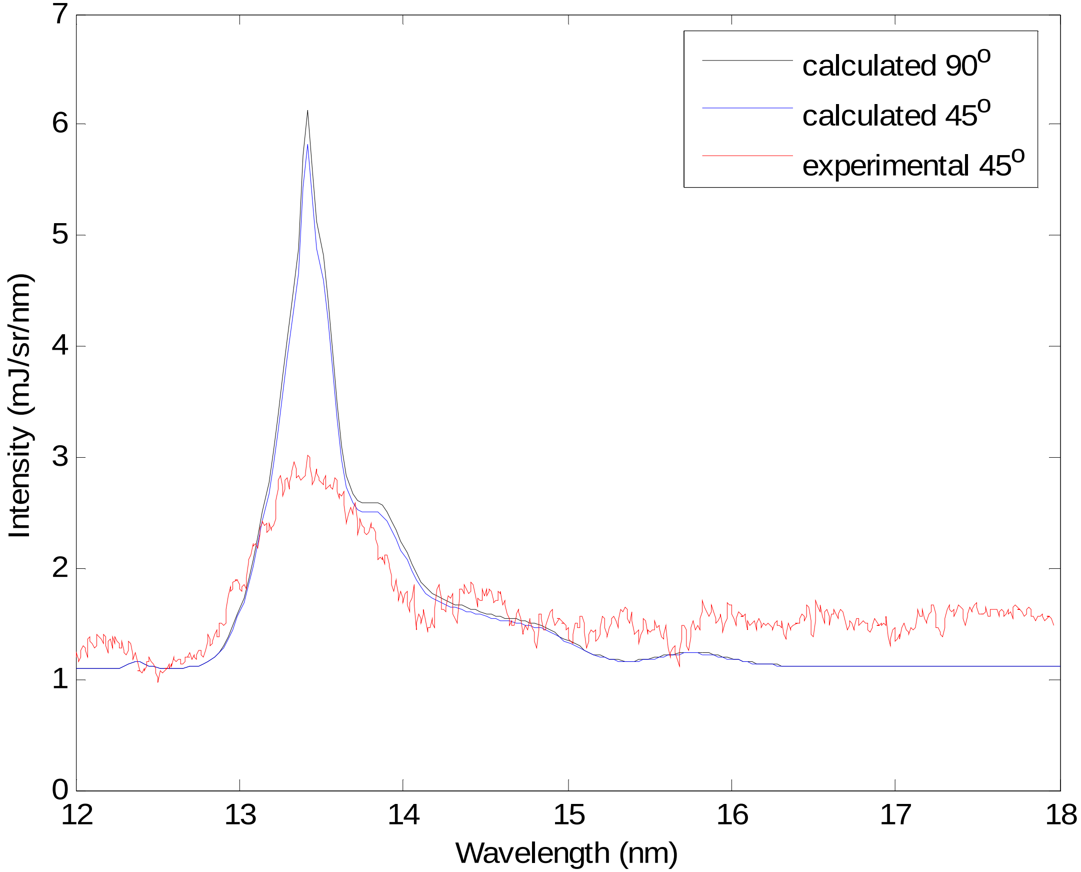

Experimental and calculated spectra

1-D plasma

✓ multi electron temperature

✓ multi electron density

✓ energy level populations

J. Appl. Phys. **99** 093302, 2006

2. Conversion efficiency

- power density survey: max CE at 0.8 x 10^{11} W/cm^2
- Lateral expansion not included!

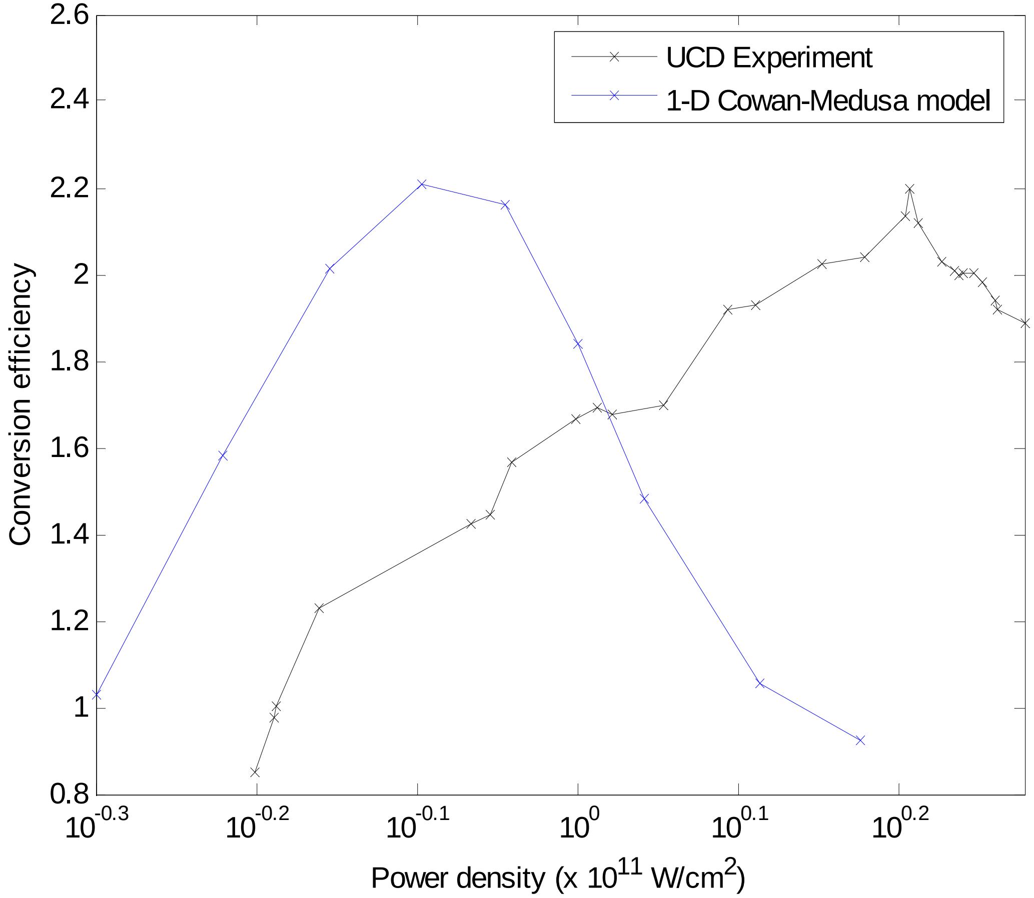

$$CE = \frac{2\pi \int \int_{13.5-1\%}^{13.5+1\%} \int_{0}^{tstop} I_{out}(\lambda, t)\, dt\, d\lambda\, dA}{E_{tot}}$$

Conversion efficiency (%) versus power density

Outline

1. A steady state plasma (optically thin)

4d-4f + 4p-4d emission: statistical UTA (*gf*), ion distribution $f_z = \mathrm{f}(T_e)$
n_e and pulse length (YAG and CO_2)

2. A time-dependent 1-D plasma (optically thick)

ion distribution, $f_z = \mathrm{f}(r,t)$, hydrodynamics [Medusa], some diagnostics
N_i, N_j level populations for radiation transport [UCD],
2 surveys: power density and pulse length (optimum laser conditions)

3. A 2-D plasma

time-dependent spectra [EPPRA, Z*]
spatial pulse shape (flat-top/Gaussian)
pulse length results

Conclusions

3. 2D plasma

Z* EPPRA

Implicit, E-L MHD, average atom code, solves ionisation kinetics self-consistently with radiation transfer

82 x 69 grid, YAG

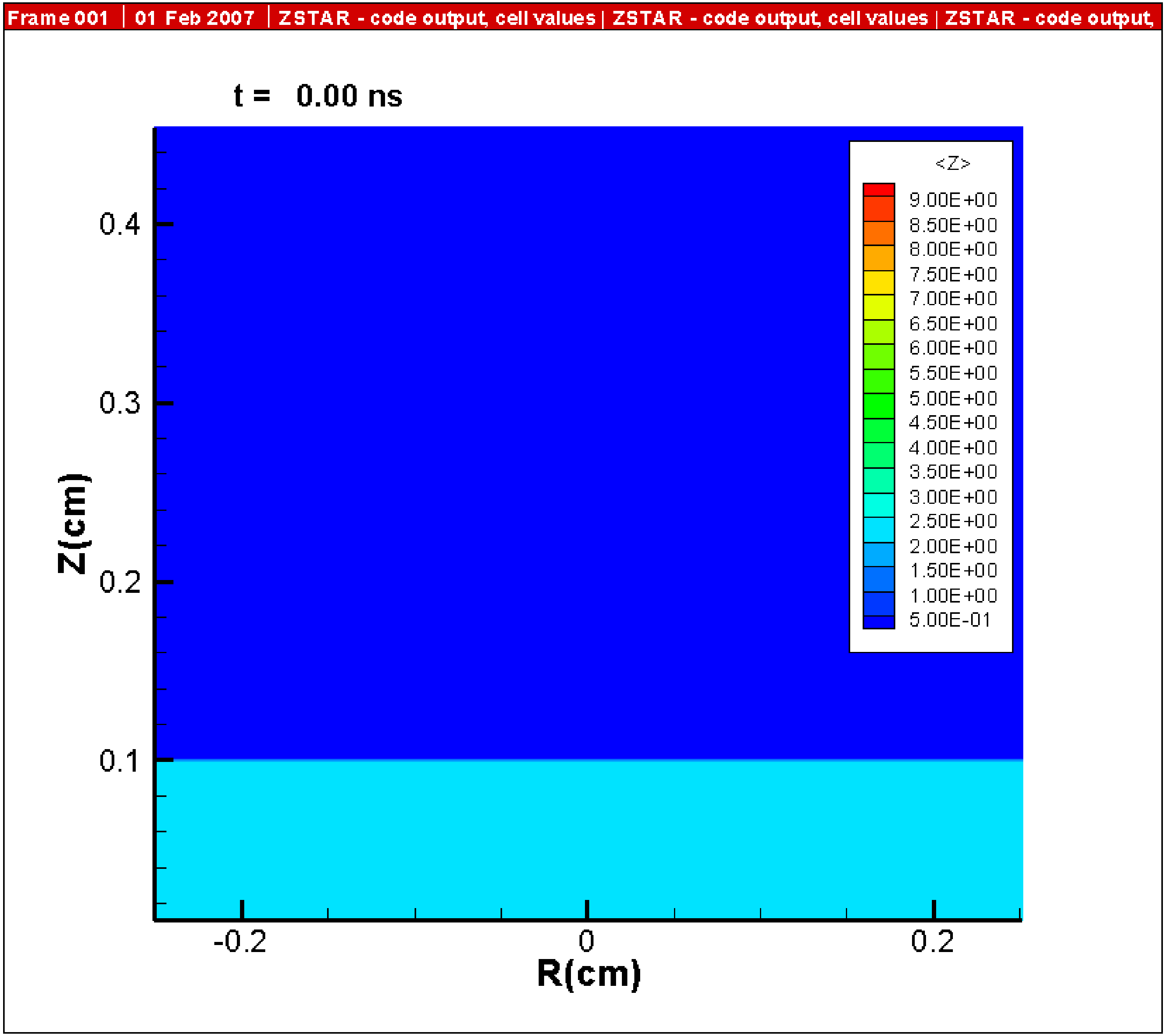

3. 2D plasma

Z* EPPRA

Implicit, E-L MHD, average atom code, solves ionisation kinetics self-consistently with radiation transfer

82 x 69 grid, YAG

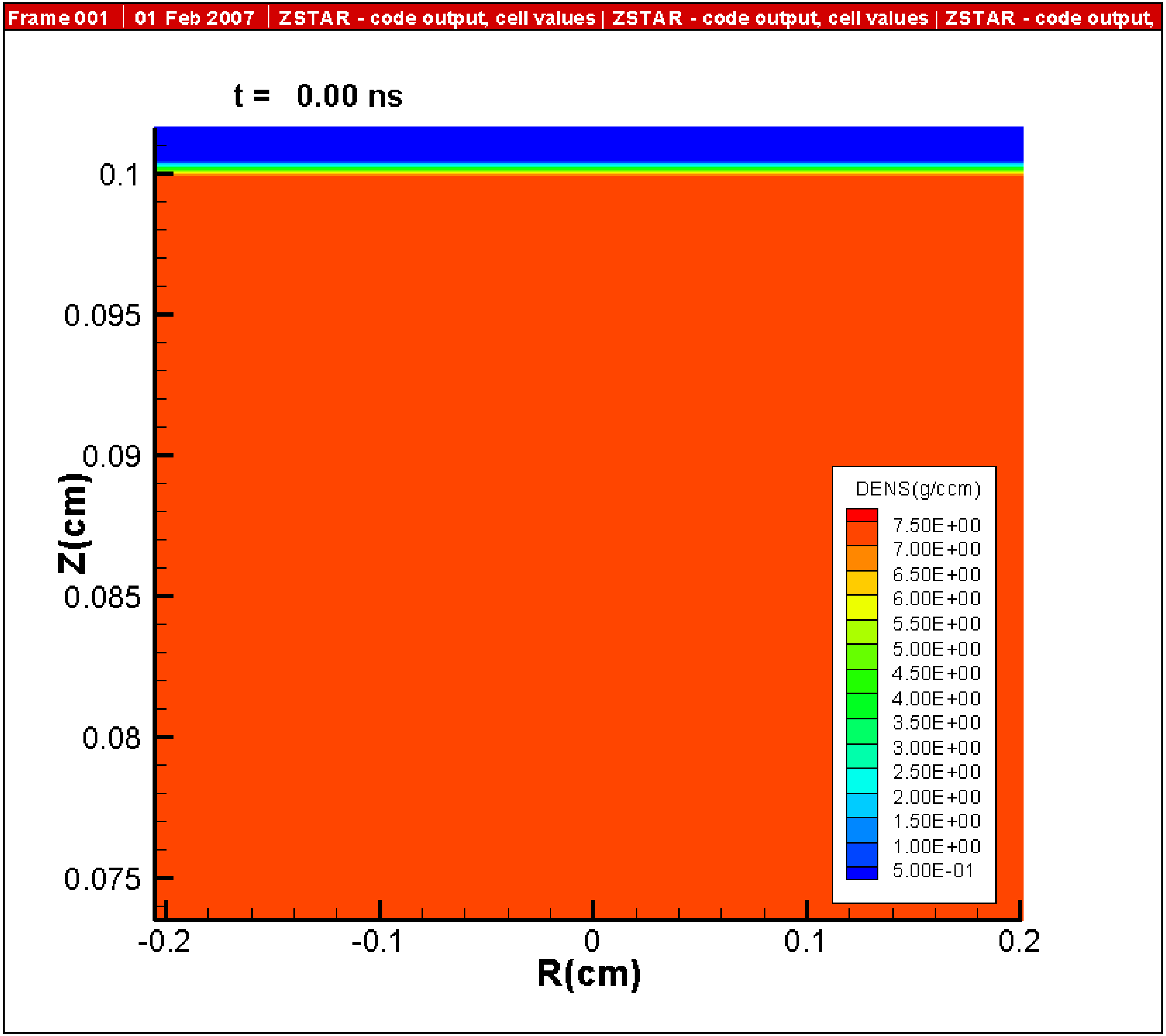

3. 2D plasma: pulse shape (spatial)

- Z* (EPPRA): 2D LPP simulation
- 2.2-ns Gaussian at peak emission

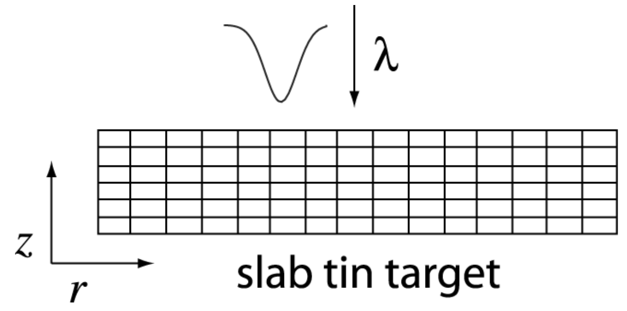

Electron temperature

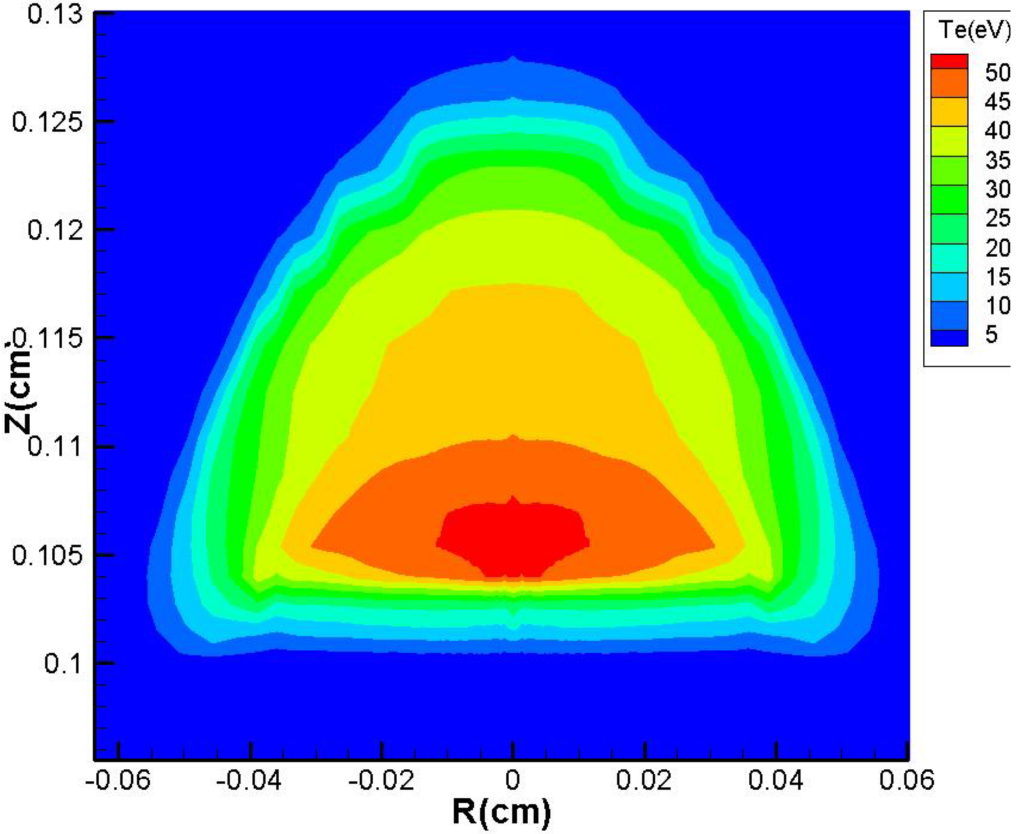

in-band emission (into 4π)

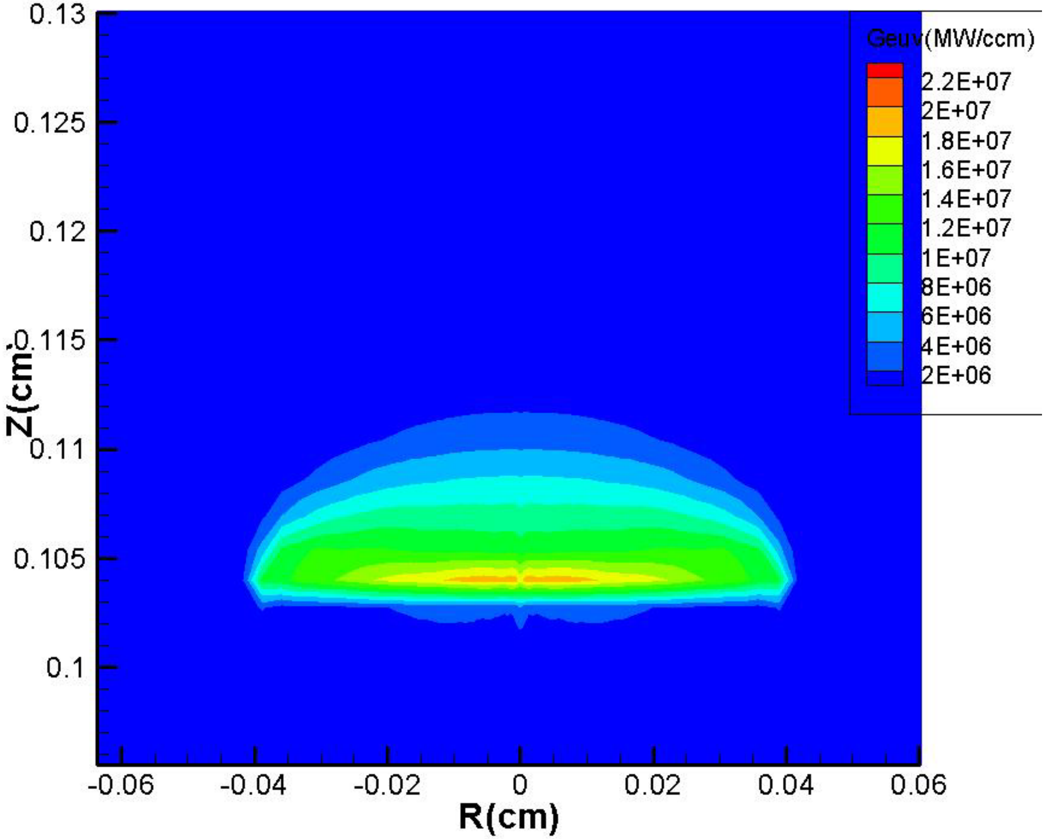

3. 2D plasma: pulse shape (spatial)

- Z* (EPPRA): 2D LPP simulation
- 2.2-ns flat-top at peak emission

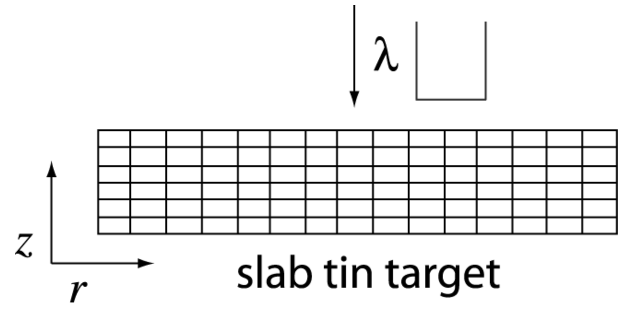

Electron temperature

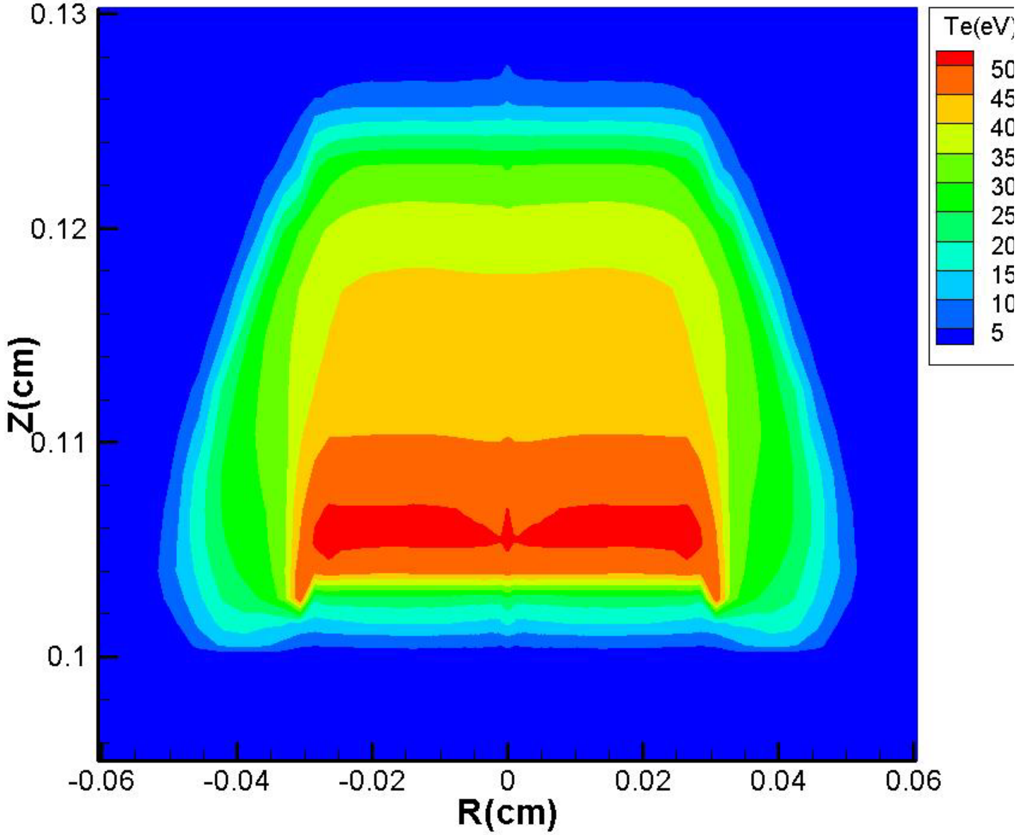

in-band emission (into 4π)

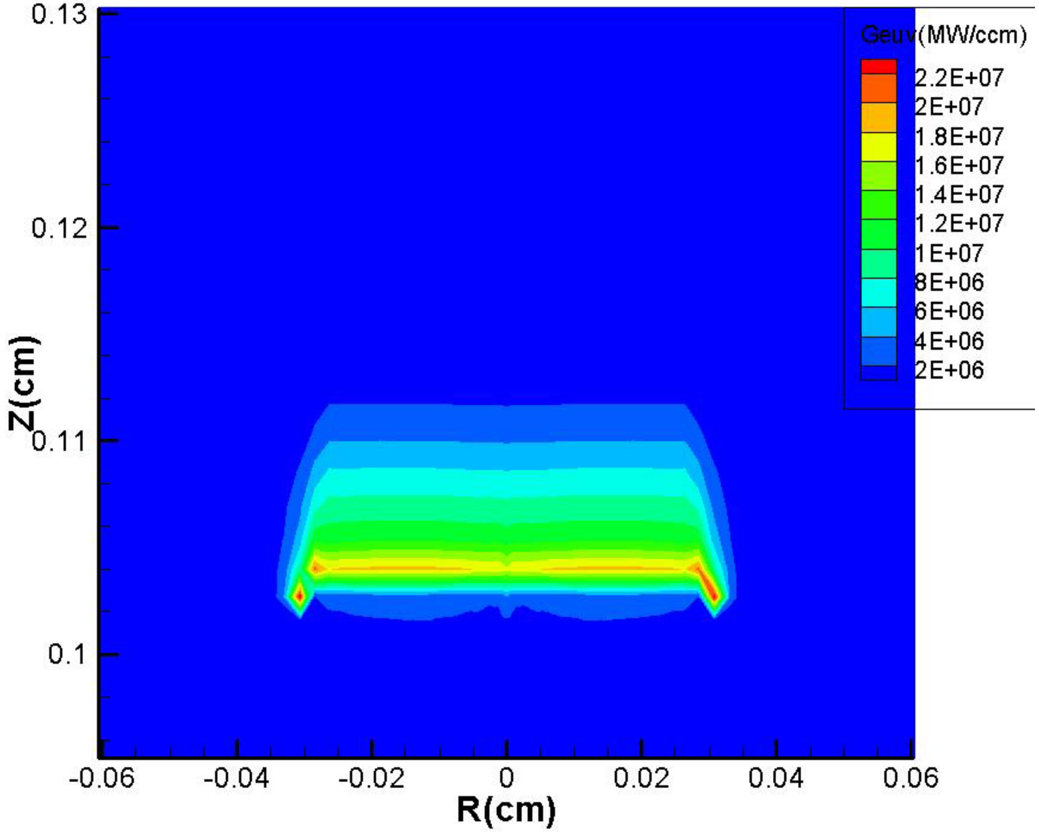

3. 2D plasma: pulse shape (spatial and temporal)

Appl. Phys. Lett., 92, 151501, 2008

- calculated Gaussian, flat-top, and experiment (Osaka ILE)
- CE versus laser power density .66 μm, ..27 μm diameter

2.2 ns

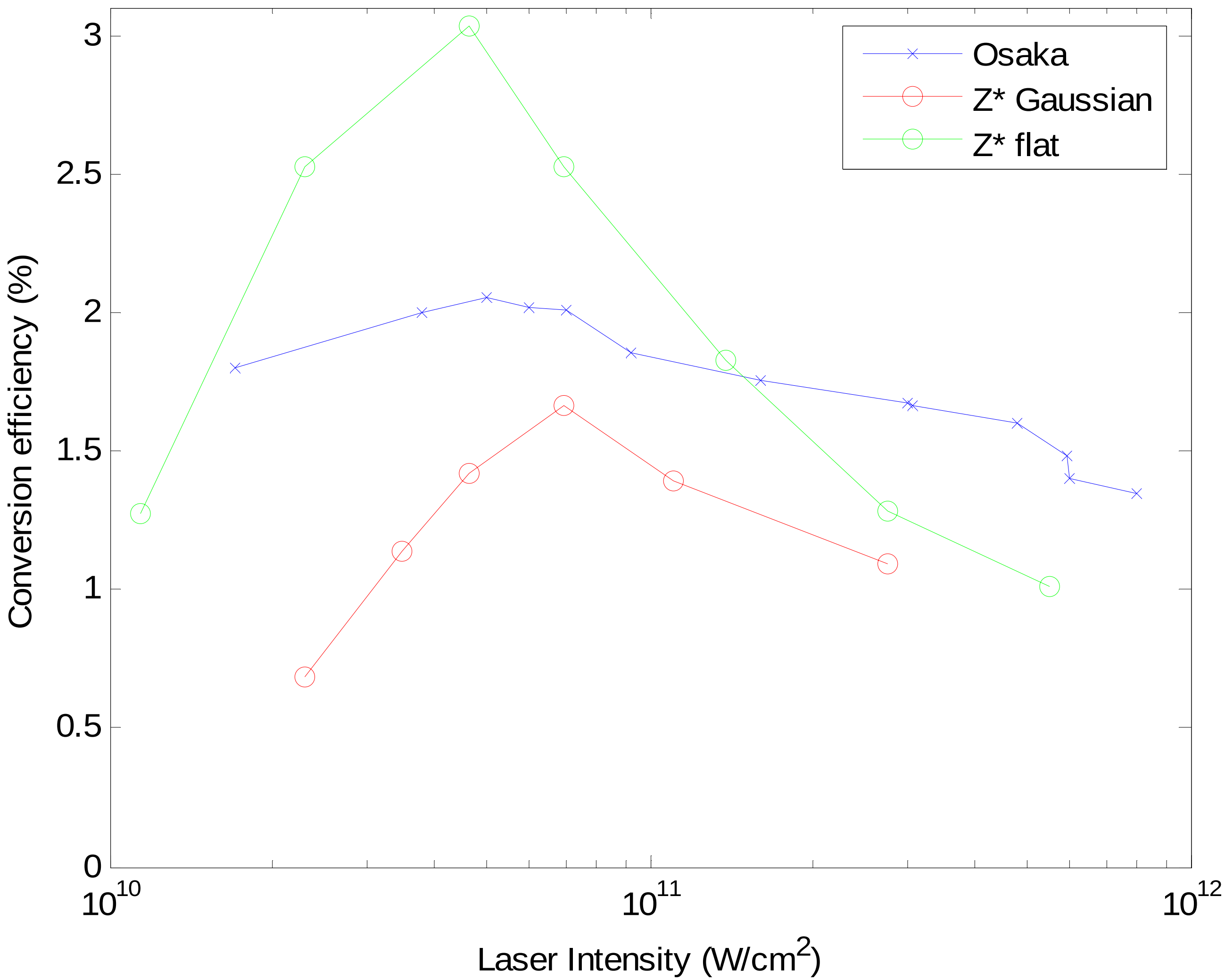

3. 2D plasma: pulse shape (spatial and temporal)

Appl. Phys. Lett., 92, 151501, 2008

- calculated Gaussian, flat-top, and experiment (Osaka ILE)
- CE versus laser power density .48 μm, .27 μm diameter

8.0 ns

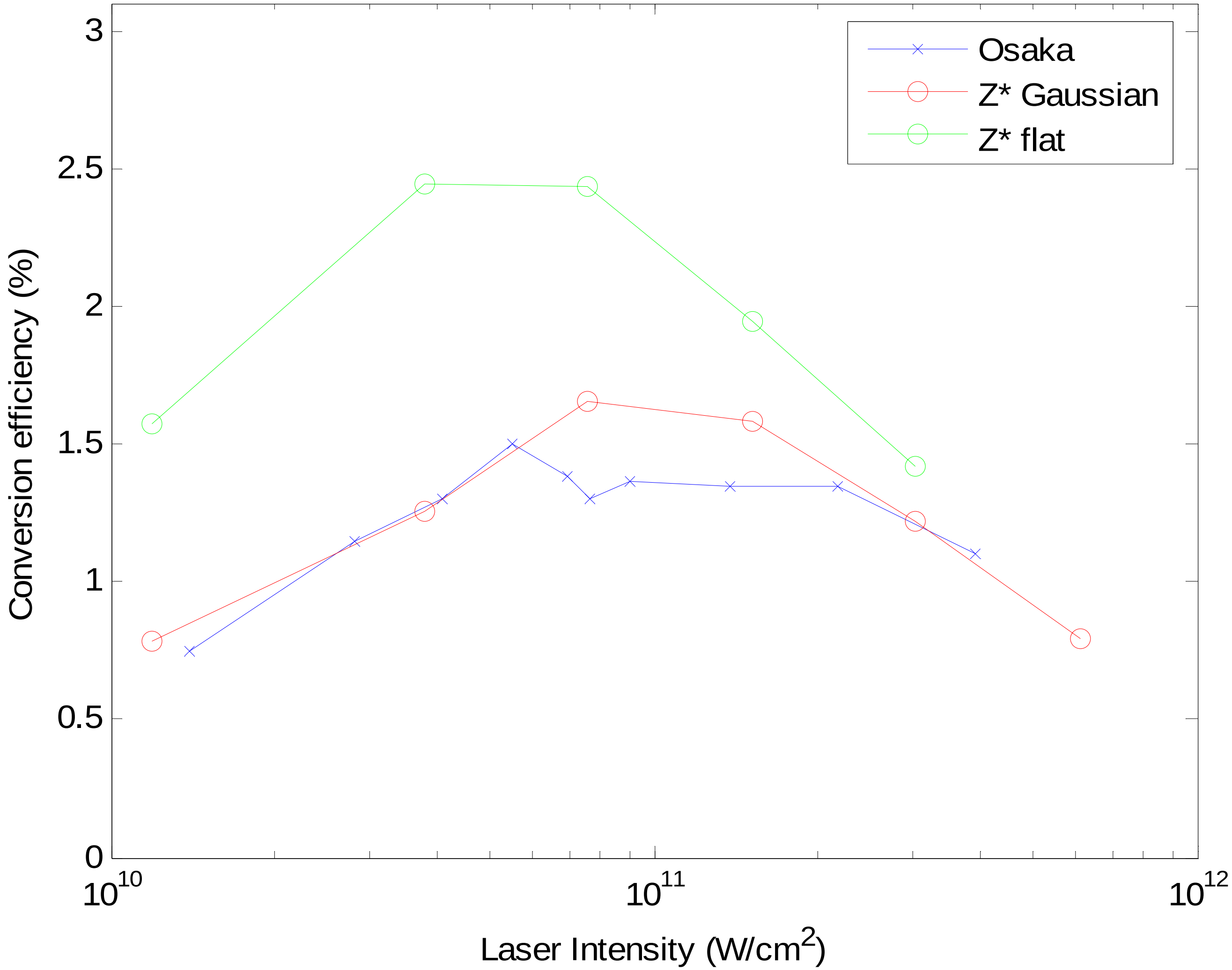

3. 2D plasma (emission lags max pulse)

- Input (laser) and output (spectral response)
- Pulse and emission curves plotted together

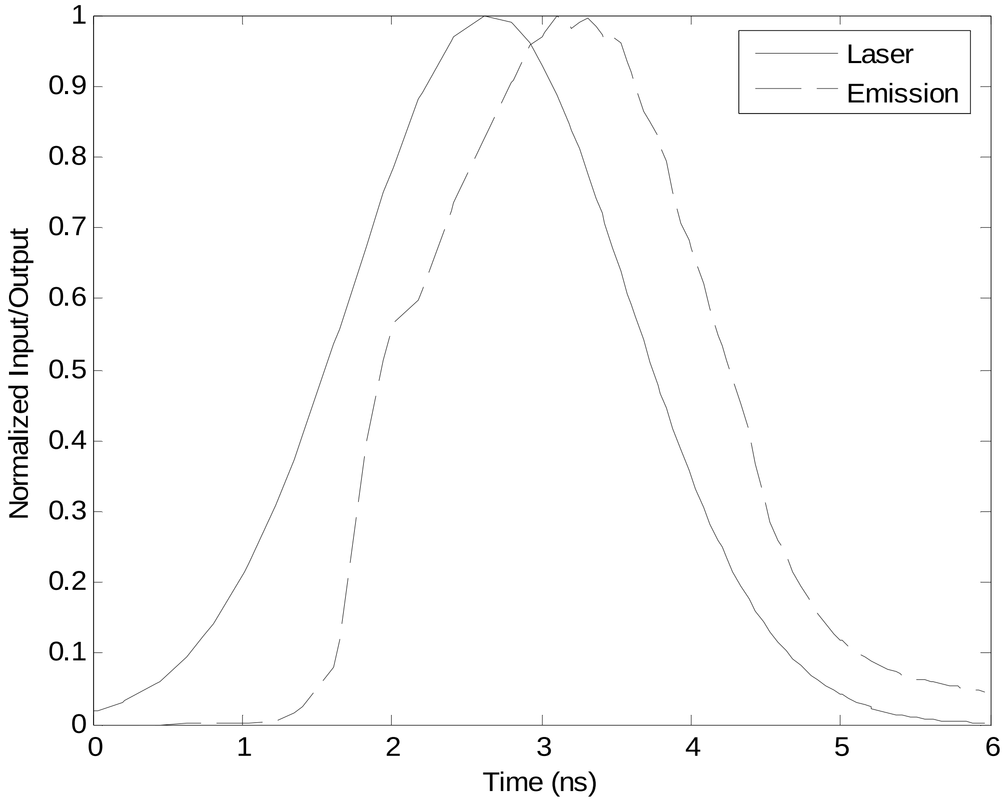

Normalized to one in-band emission and laser power versus time.

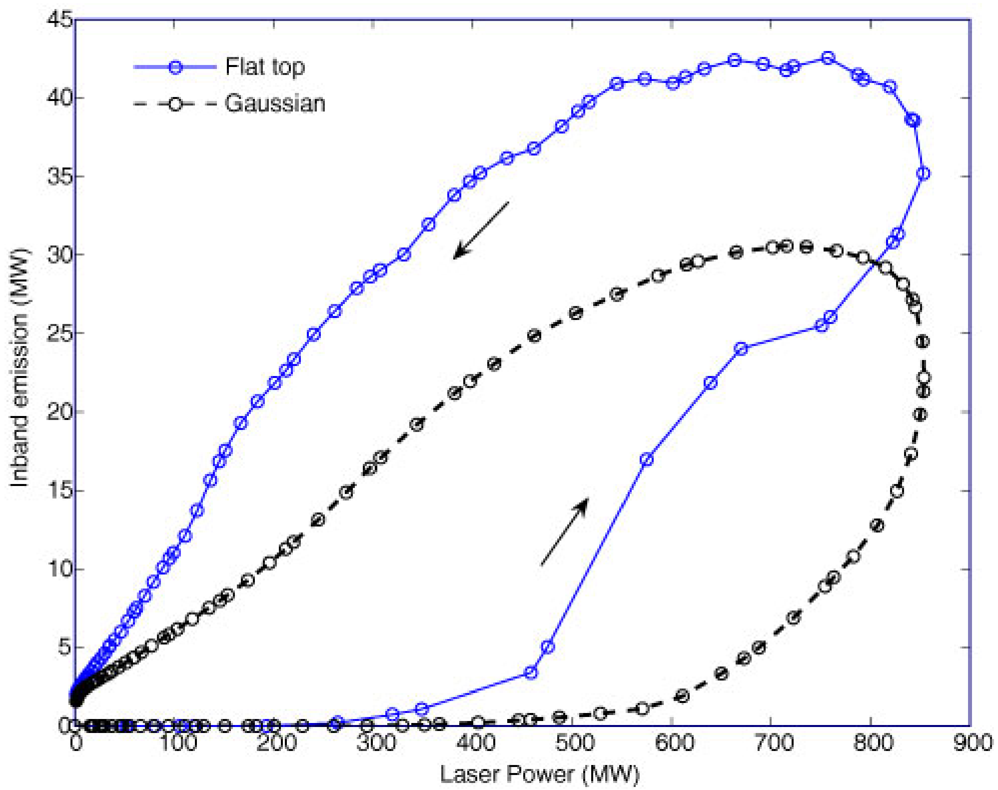

In-band emission (into 4π) versus laser power for different beam profiles (flat-top in blue and Gaussian in black).

Conclusions

- steady-state (optically thin) plasma:
  - statistical model: source brightness $F \rightarrow$ 40 eV
- time-dependent plasma (optically thick):
  - energy functional for UTAs $\rightarrow$ more manageable computation!
  - radiation transport but no lateral expansion
  - max CE $\rightarrow$ 0.8×10^{11} W/cm^2 and 10 ns.
- What's next?
  - CO_2 modelling, pulse shaping, and pre-pulse-pulse

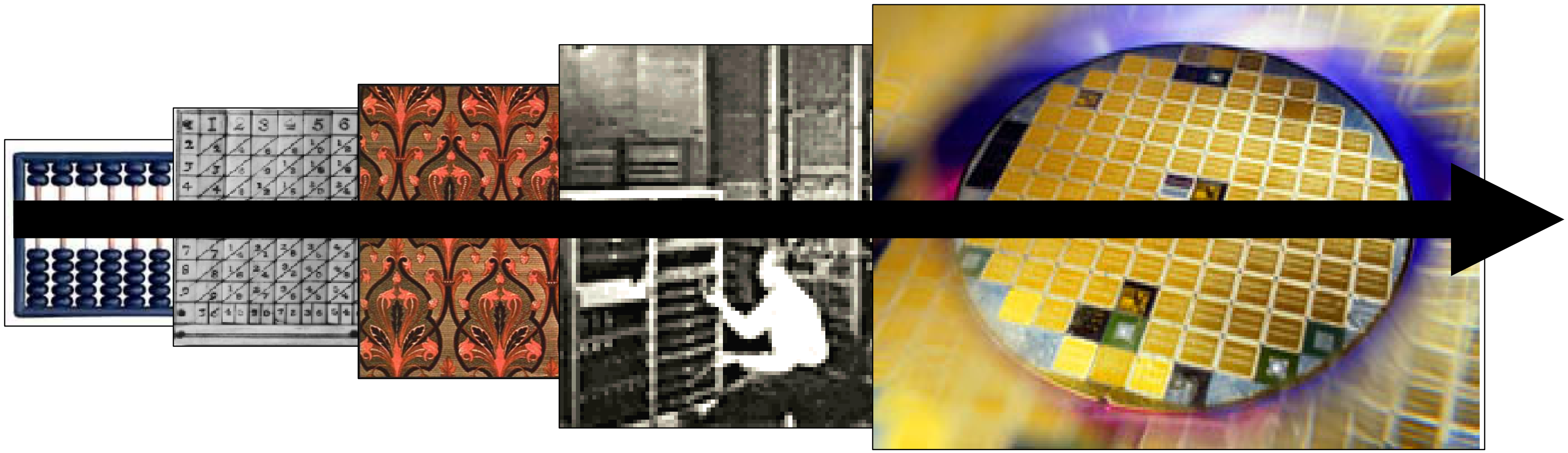

Some recent references

"Tin laser-produced plasma source modelling at 13.5 nm for extreme ultraviolet lithography," J. White, G. O'Sullivan, S. Zakharov, P. Choi, V. Zakharov, H. Nishimura, S. Fujioka, and K. Nishihara, *Appl. Phys. Lett.*, 92, 151501, 2008

"Optimising 13.5-nm laser-produced tin plasma emission as a function of laser wavelength," J. White, P. Dunne, P. Hayden, F. O'Reilly, and G. O'Sullivan, *Appl. Phys. Lett.*, 90, 181502, 2007.

"Simplified calculation of non-local thermodynamic equilibrium excited state populations contributing to 13.5-nm emission in a tin plasma" J. White, A. Cummings, P. Dunne, P. Hayden, and G. O'Sullivan *J. Appl. Phys.* **101** 043301, 2007

"13.5 nm extreme ultraviolet emission from tin based laser produced plasma sources" P. Hayden, A. Cummings, N. Murphy, G. O'Sullivan, P. Sheridan, J. White, and P. Dunne, *J. Appl. Phys.* **99** 093302, 2006

"Tin based laser-produced plasma source development for EUVL" P. Hayden, J. White, A. Cummings, P. Dunne, M. Lysaght, N. Murphy, P. Sheridan and G. O'Sullivan. *Microelectronic Engineering* 83, 699, 2006

"A spatio-temporal study of variable composition laser –produced tin plasmas" A. Cummings, G. O'Sullivan, P. Dunne, E. Sokell, N. Murphy, J. White, P. Hayden, P. Sheridan, M. Lysaght and F. O'Reilly *J. Phys. D: Appl. Phys.* **39** (1) 73-93, 2006

"**Atomic physics of highly charged ions and the case for Sn as a source material**" G. O'Sullivan, A. Cummings, P. Dunne, P. Hayden, L. McKinney, N. Murphy and J. White. Ch. 5. in *"EUV Sources for Lithography"* editor Vivek Bakshi, Publ. SPIE, 2006

"**Tin based plasmas as EUV sources for 13.5 nm lithography: a statistical approach**" J. White, P. Hayden, P. Dunne, A. Cummings, N. Murphy, P. Sheridan and G. O'Sullivan *J. Appl. Phys.* **98** 113301, 2005

UCD Modelling Collaborations

DCU

John Costello, Paddy Hayden, Pat Yeates

突破EUV光源的瓶颈

Chenzong Dong, Mao Gen Su

David Ruzic

H. Nishimura, S. Fujioka,
K. Nishihara

EPPRA

Sergey Zakharov, Vasily Zakharov, Peter Choi

AIXUV EUV-Technology

Rainer Lebert

intel

SEMATECH

Accelerating the next technology revolution.

UCD Spectroscopy

Spectroscopy of atoms and ions in laser-produced plasmas.
Atomic structure calculations.
Laser produced plasmas for EUV light source lithography.
Spatial and temporal analysis of laser plasmas.
Statistics of complex level structure and spectra.
Synchrotron-based photoelectron spectroscopy.
Photoabsorption of ions.

Gerry O'Sullivan
Rebekah D'Arcy
Padraig Dunne
Kenneth Fahy
Colm Harte
Oran Morris
Tom McCormack
Aodh O'Connor
Fergal O'Reilly
Paul Sheridan
Emma Sokell
Eileen Weadick
John White

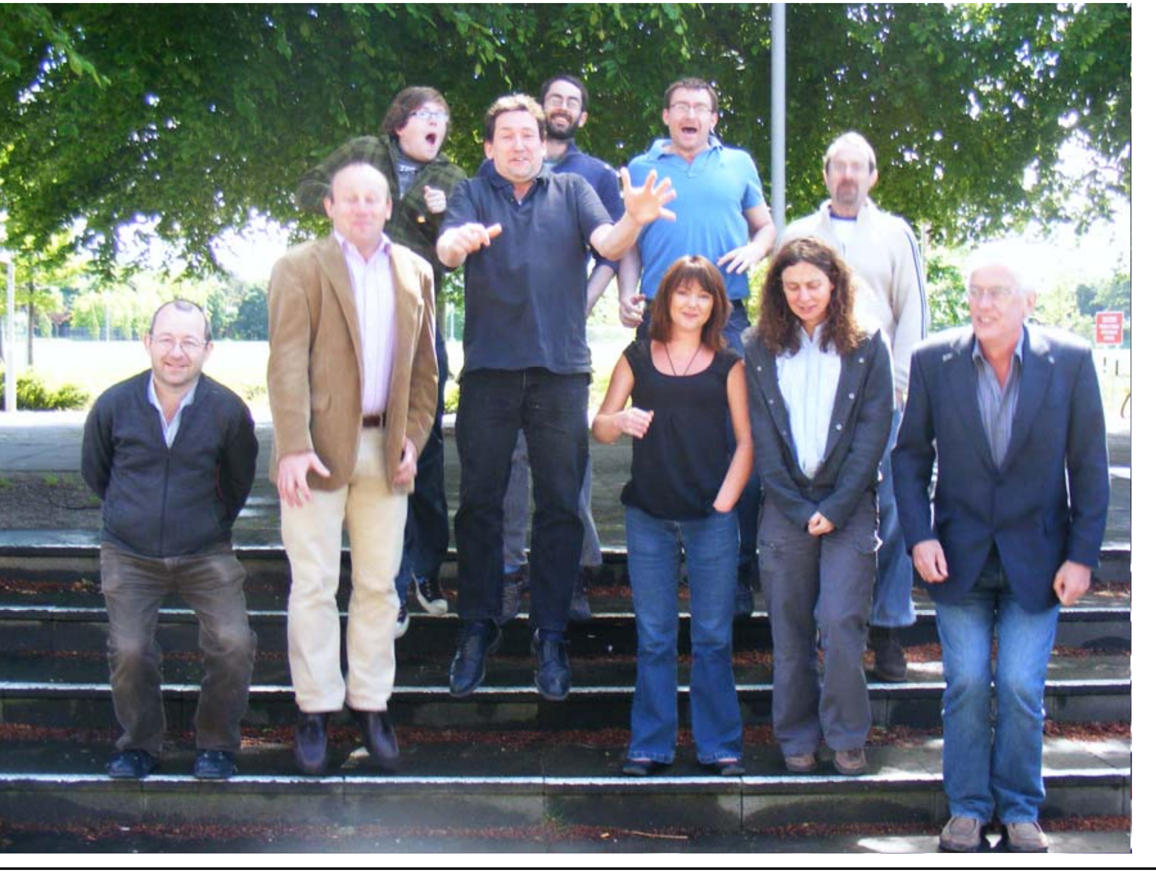

Baltimore

- Baron Baltimore (a.k.a. Lord Baltimore)
- Baile an Tí Mhóir and Dún na Séad